Temperature versus salinity gradients below the ocean mixed layer

Robert W. Helber,[1] A. Birol Kara,[1,2] James G. Richman,[1] Michael R. Carnes,[1] Charlie N. Barron,[1] Harley E. Hurlburt,[1] and Timothy Boyer[3]

Received 17 June 2011; revised 22 December 2011; accepted 16 March 2012; published 3 May 2012.

[1] We characterize the global ocean seasonal variability of the temperature versus salinity gradients in the transition layer just below the mixed layer using observations of conductivity temperature and depth and profiling float data from the National Ocean Data Center's World Ocean Data set. The balance of these gradients determines the temperature versus salinity control at the mixed layer depth (MLD). We define the MLD as the shallowest of the isothermal, isohaline, and isopycnal layer depths (ITLD, IHLD, and IPLD), each with a shared dependence on a 0.2°C temperature offset. Data are gridded monthly using a variational technique that minimizes the squared analysis slope and data misfit. Surface layers of vertically uniform temperature, salinity, and density have substantially different characteristics. By examining differences between IPLD, ITLD, and IHLD, we determine the annual evolution of temperature or salinity or both temperature and salinity vertical gradients responsible for the observed MLD. We find ITLD determines MLD for 63% and IHLD for 14% of the global ocean. The remaining 23% of the ocean has both ITLD and IHLD nearly identical. It is found that temperature tends to control MLD where surface heat fluxes are large and precipitation is small. Conversely, salinity controls MLD where precipitation is large and surface heat fluxes are small. In the tropical ocean, salinity controls MLD where surface heat fluxes can be moderate but precipitation is very large and dominant.

Citation: Helber, R. W., A. B. Kara, J. G. Richman, M. R. Carnes, C. N. Barron, H. E. Hurlburt, and T. Boyer (2012), Temperature versus salinity gradients below the ocean mixed layer, *J. Geophys. Res.*, *117*, C05006, doi:10.1029/2011JC007382.

1. Introduction

[2] The ocean mixed layer is understood to represent the top portion of the ocean surface boundary layer where vertically uniform seawater properties are dominated by three-dimensional turbulent flow. The total depth of the surface boundary layer extends deeper than the mixed layer. While the concept of the mixed layer is simple, its quantification has prominence in oceanographic research (see *Kantha and Clayson* [2000] for a review). In addition, observing and modeling the ocean mixed layer is complex where the details of the turbulence modeling and the mixed layer definition can have a large impact [*Kara et al.*, 2010]. One particular complexity of the mixed layer stems from the fact that seawater density is primarily influenced by two disunited quantities, temperature and salinity. In the present article, we take a generalized approach making temperature and salinity co-variability central to an investigation of the global ocean mixed layer using observations of conductivity, temperature, and depth (CTD) and profiling float data from the National Ocean Data Center's (NODC) World Ocean Data set (WOD) 2009.

[3] Investigation of the mixed layer will focus on the gradients at the base of the mixed layer in attempt to identify whether temperature or salinity is the component of seawater that delineates the mixed layer depth (MLD). Investigating the controlling factor of the MLD requires that we also consider the transition layer, which is the part of the ocean surface boundary layer below the mixed layer and above the relatively quiescent ocean interior. We denote our estimate of the transition layer thickness as TLT.

[4] In the present article, we first discuss the current knowledge of temperature versus salinity control of the ocean mixed layer and the importance of the transition layer (section 2). The methods we use for the present analysis stem from a new definition of MLD that differs slightly from that in the current scientific literature (see sections 4). The resulting analysis is tailored to address the following main questions:

[5] (1) Where in the global ocean during the annual cycle is the MLD determined by gradients of either temperature or salinity? (2) Where in the global ocean during the annual cycle do transition layer gradients of temperature and salinity occur at the same depth? (3) What are some likely processes responsible for the temperature or salinity control of the

[1]Oceanography Division, Naval Research Laboratory, Stennis Space Center, Mississippi, USA.
[2]Deceased 14 September 2009.
[3]National Oceanographic Data Center, NOAA, Silver Spring, Maryland, USA.

MLD? (4) Where in the global ocean during the annual cycle does large variability and noise sensitivity increase the uncertainty of the ocean MLD climatology? (5) How does vertical resolution of in situ profile observations impact estimates of the MLD and transition layer thickness?

[6] After the background material in section 2, section 3 has a description of the observations data set. The methods described in section 4 include estimating surface layer depths of vertically uniform temperature, salinity, and density, the transition layer thickness, resolution, noise sensitivity analysis, and gridding techniques. Section 5 describes typical profile characteristics from around the world, and section 6 describes the MLD climatology. Section 7 contains the density control analysis where the first two main questions of this analysis are addressed. Estimates of the transition layer thickness are in sections 8 and 9 contains the summary and conclusions.

2. Background

[7] It has long been recognized that both salinity and temperature can provide the dominant gradient at the base of the mixed layer [*de Boyer Montégut et al.*, 2007], determining the mixed layer depth (MLD). For most of the world's oceans, the MLD is determined by temperature. Ocean regions where salinity controls the depth of the mixed layer are understood to have "barrier" layers [*Lukas and Lindstrom*, 1991], where the depth of vertically uniform temperature exceeds the depth of vertically uniform density and salinity. In this case, salinity determines the depth of the mixed layer due to a relatively large gradient in salinity at the MLD. Another commonly studied layer is known as the "compensated" layer, where temperature and salinity vertical gradients balance in their effect on density, resulting in a layer of uniform density that extends deeper than layers of vertically uniform temperature and salinity.

[8] A considerable amount of research has been conducted describing "barrier" layer variability [e.g., *Kara et al.*, 2000b; *Mignot et al.*, 2009], because it has substantial implications for air-sea interactions and climate [e.g., *Liu et al.*, 2009]. The factors that control the mixed layer and the temperature versus salinity variability can be described using the temperature and salinity conservation equations [e.g., *Feng et al.*, 2000] given by

$$\overbrace{Q_0 - R_S\Big|_{-MLD}}^{\text{surface forcing}} = \overbrace{\int_{-MLD}^{0} \rho_0 c_P \frac{\partial T}{\partial t} dz - F_T\Big|_{-MLD}}^{\text{1D processes}} + \overbrace{\int_{-MLD}^{0} \rho_0 c_P (\mathbf{u} \cdot \nabla T) dz}^{\text{advection}}, \tag{1a}$$

$$S_0(E-P) = \int_{-MLD}^{0} \frac{\partial S}{\partial t} dz - F_S\Big|_{-MLD} + \int_{-MLD}^{0} (\mathbf{u} \cdot \nabla S) dz. \tag{1b}$$

The terms are separated into three categories: surface forcing on the left side, one dimensional subsurface processes in the middle, and advection on the far right. The surface forcing for temperature conservation in equation (1a) includes the net surface heat flux, Q_0, minus the part of the penetrating solar radiation that exits the mixed layer at the MLD, $R_S|_{-MLD}$. On the right side of equation (1a) we have temperature tendency, $\int_{-MLD}^{0} \rho c_P \partial T/\partial t dz$, which is a measure of the heat increase or decrease within the mixed layer minus the turbulent heat flux at the base of the mixed layer, $F_T|_{-MLD}$. The symbol ρ_0 represents a reference density, and c_P represents specific heat capacity of seawater at constant pressure. The partial derivative of temperature is integrated from the surface at $z = 0$ to the mixed layer depth $z = -MLD$. Temperature tendency and vertical turbulent heat flux are considered one dimensional process. The three-dimensional process on the far right in equation (1a) is advection and is the heat flux due to horizontal and vertical velocity, where $\mathbf{u}$ is a three dimensional vector with velocities u, v, and w, in the zonal, meridional, and vertical direction respectively. The dot product of $\mathbf{u}$ and ∇T is integrated from the surface at $z = 0$ to the mixed layer depth $z = -MLD$. The left hand side of the salinity conservation equation (1b) is a salt flux per unit time given by $S_0(E - P)$, which is proportional to evaporative flux E minus precipitation P, where S_0 is the surface salinity. The terms on the right hand side of equation (1b) are analogous to those in equation (1a) but for salinity.

[9] Since the present analysis is global on seasonal timescales, the terms we discuss in the results sections will pertain mostly to the left hand side of equations (1a) and (1b). Where $E - P$ is large in the absence of large surface heat flux, Q_0, we would expect salinity to be the controlling gradient at the base of the mixed layer. This is expected because where Q_0 is small, temperature fluxes at the MLD, $R_S|_{-MLD}$ and $F_T|_{-MLD}$, are also likely to be small, on average. Therefore, large vertical temperature gradients are not likely to exist. Since, $E - P$ is large, salinity is likely to be the controlling factor for MLD. Conversely, where $E - P$ is small and the surface heat flux is large, we may expect to see temperature control the MLD. This is because without a freshwater input, salinity is not likely to have large vertical gradients. From limited observations, it is generally not possible to know the effect temperature and salinity tendency and adjective fluxes. Where possible, the likely influence of surface fluxes Q_0 versus freshwater input $E - P$ will be discussed in sections 5, 6, and 7.

[10] In the present article, the MLD is defined as the minimum depth among the isopycnal, isothermal, and isohaline layer depths, as described below in section 4. As a result of this definition, barrier and compensated layers are part of the transition layer below the mixed layer, but still part of the upper ocean boundary layer. In order to determine whether temperature or salinity is controlling the depth of the mixed layer, the present analysis describes the top of the transition layer. While the global mixed layer is a well defined and popular topic of research, studies of the transition layer have been regional [e.g., *Johnston and Rudnick*,

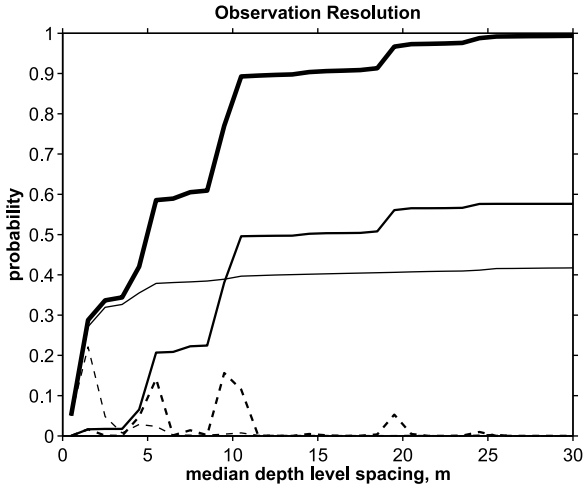

Figure 1. The solid lines are the cumulative probability of median profile depth level spacing in 1 m bins. The dashed lines are the probabilities for binned median profile depth level spacing. The thin, medium and thick lines are for CTDs, Argo floats, and both CTD and floats combined, respectively.

2009] and the global variability has not been adequately described.

[11] The transition layer is of particular interest because it links the well mixed surface layer to the ocean interior. While seawater properties in the ocean mixed layer are vertically uniform, density gradients exist at all scales of variability in the horizontal. For example, *Rudnick and Martin* [2002] have shown that the ocean mixed layer at sub-mesoscales is horizontally well density compensated. Below the mixed layer in the transition layer or the thermocline, the density structure is less horizontally compensated. Density compensation is thus altered as seawater evolves along pathways from the mixed layer through the thermocline and understanding this processes is an active topic of research [e.g., *Ferrari and Paparella*, 2003]. A goal of the present article is to characterize the global seasonal variability of the observed temperature versus salinity vertical gradients in the transition layer just below the mixed layer.

[12] The vertical density compensation below the mixed layer varies around the world as observed in the trend of thermosteric versus halosteric sea level that varies with latitude and ocean [*Levitus et al.*, 2005]. Variability of thermosteric versus halosteric sea level occurs primarily in the transition layer, because the largest vertical gradients are found there. Vertical density compensation is also connected with injections of spice in the subtropics associated with interannual isopycnal climate variability [*Yeager and Large*, 2007]. Other research suggests that horizontal density compensation has a role in the effectiveness of eddy heat transport where mean geostrophic currents cross the mean isotherms in the south Pacific beneath the Peru-Chile stratus cloud cover [*Zheng et al.*, 2010].

[13] The effects of density compensated gradients below the mixed layer are not limited to ocean circulation and climate. Since sound speed and density have different sensitivities to temperature and salinity, the acoustic and hydrodynamic variability of the upper ocean can diverge [*Helber et al.*, 2008] primarily in regions of the ocean where vertical density compensation occurs.

[14] In this paper we investigate the mixed layer depth (MLD) and transition layer thickness (TLT) as observed from a global data set of temperature and salinity profiles of relatively coarse vertical resolution (1–10 m), compared to microstructure measurements [e.g., *Brainerd and Gregg*, 1995]. The advantage of working with coarse resolution profiles is that they are relatively abundant and available from all parts of the global ocean [*Boyer et al.*, 2009]. Since the observations do not resolve horizontal scales of variability, we focus on the vertical structure of the upper ocean.

3. Data

[15] The observational data are from the National Ocean Data Center's (NODC) World Ocean Data set (WOD) 2009 [*Boyer et al.*, 2009]. We use temperature (T) and salinity (S) paired profiles from profiling floats (Argo) [e.g., *Roemmich and Gilson*, 2009] and conductivity, temperature and depth (CTD) probes. The purpose is to have a global set of paired temperature and salinity observations to diagnose the MLD and the density compensation characteristics of the transition layer.

[16] We hypothesize that the vertical resolution of the observation profiles will substantially impact the estimates of the MLD and transition layer thickness. Figure 1 shows that the median depth level spacing of CTD and Argo profiles are substantially different. The probability and cumulative probability are constructed for profiles from the surface to 600 m or the deepest level in the profile, whichever comes first. All profiles must also have the shallowest measurement level above 12 m depth. There also must be at least 10 levels in the upper 120 m of the profile. All profiles have a salinity paired with each temperature. The total numbers of profiles that qualify are 466,790 Argo floats and 340,531 CTDs, for a total of 807,321 profiles. Most CTDs have a depth level spacing between 1 and 2 m. Floats have either 5 or 10 m depth level spacing. There are a small number of Argo profiles with approximately 2.5 m resolution (14,126). These are new Argo floats equipped with Iridium communication systems, which allow more data to be transmitted while the float is at the surface.

[17] To investigate the impact of vertical resolution on estimating the MLD and transition layer we separate the data into high and low resolution subsets. The high resolution subset consists of 277,161 profiles (CTDs) that have vertical depth spacing of 3 m or less (Figure 2, top). The global sampling is densest in the North Atlantic, near the coasts, along shipping lanes, and along WOCE hydrographic and TAO mooring lines. In the vast majority of 1/4° boxes, there are less than 10 high resolution CTD profiles available.

[18] All available (833,995) paired temperature and salinity profiles provide vastly superior geographical coverage (Figure 2, bottom). On the observation levels, the data is a conglomerate of low and high vertical resolution profiles. The CTDs tend to have a vertical resolution of approximately 1 m while the Argo profiles have a vertical resolution of 5 or 10 m (Figure 1). As will be shown in section 3.4, MLD estimates have a low bias when computed from low resolution profiles. To create a consistent set of observations,

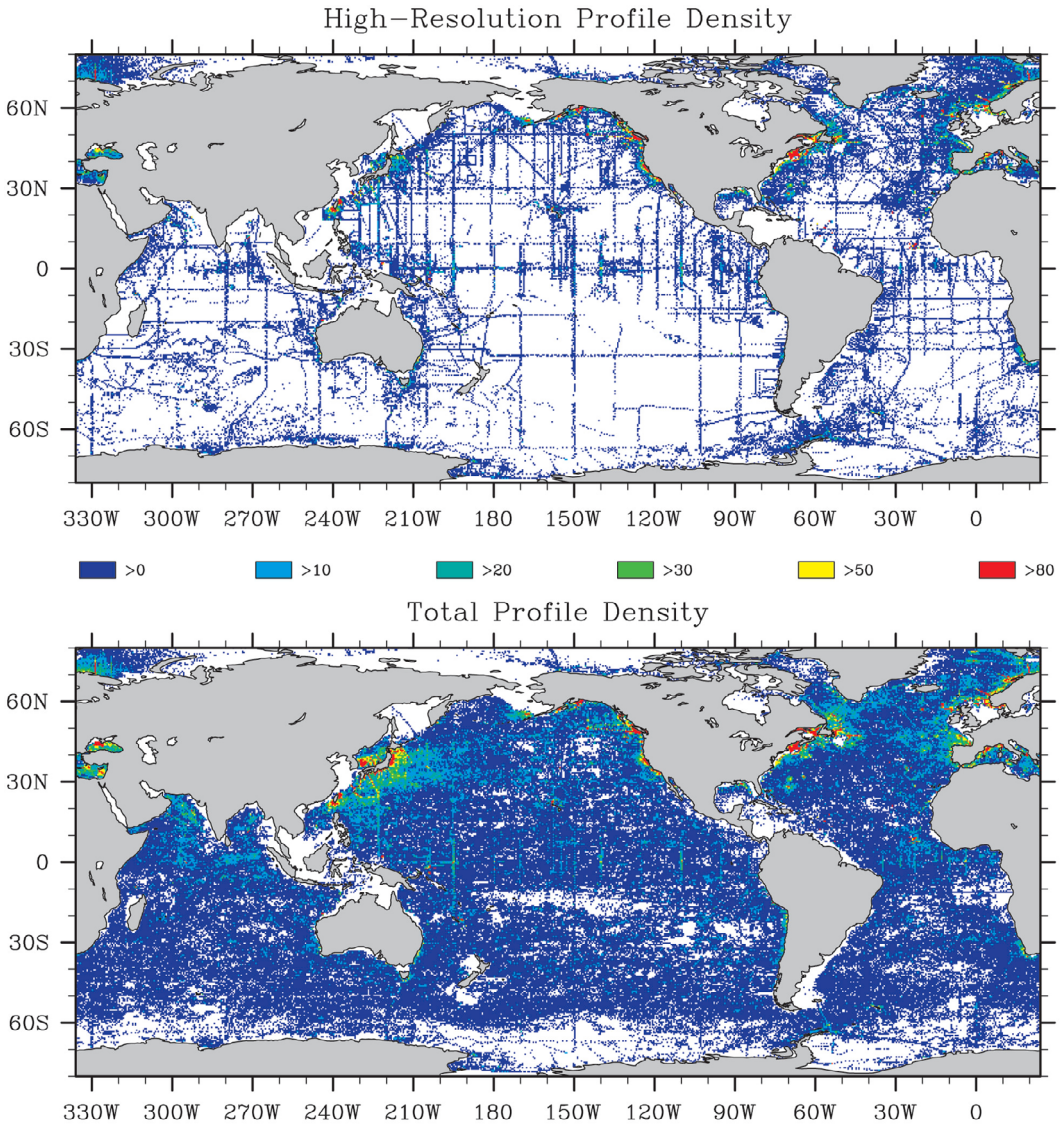

Figure 2. The density of temperature and salinity profile observations in 1/4° bins for (a) observations with vertical spacing less than 3 m (277,161), and (b) all profiles of any vertical resolution (833,995).

we sub-sample the high resolution CTDs and interpolate to the depth sampling of a typical Argo profile starting at 5 m with 10 m depth spacing to produce the largest consistently sampled data set with good geographical coverage. Since the salinity sensor on the Argo profiles must be turned off before the surface is reached, the shallowest value obtained in an Argo profile is at approximately 4 m. All values below 4 m are spaced by approximately 10 m. The re-sampled data set, with Argo-like vertical sampling, provides a view of the ocean as observed consistently at 10 m depth level spacing.

4. Methods

4.1. Vertically Uniform Layer Depths

[19] MLD is estimated from in situ profiles utilizing an approach that independently incorporates temperature, salinity, and density profiles. Since the MLD represents an isotropic turbulent layer, temperature, salinity, and density should all be vertically uniform in the mixed layer. Analysis of in situ profiles reveals that the isothermal, isohaline, and isopycnal layer depths (ITLD, IHLD, and IPLD, respectively) are often different. We define the MLD, as estimated from in situ profiles, as the shallowest of the three layer depths, ITLD, IHLD, or IPLD. As a result, the MLD is vertically uniform, and barrier and compensated layers fall within the transition layer.

[20] Traditionally, MLD is defined as the IPLD. We depart from this definition to more consistently treat cases where density compensation produces IPLD deeper than either the ITLD or the IHLD. The IPLD can extend deeper than both the ITLD and the IHLD when vertical trends in temperature and salinity result in opposing contributions to the density gradient. These conditions are associated with spice [e.g., *Flament*, 2002] variability where either hot-and-salty or cold-and-fresh water property changes result in constant density.

Table 1. Surface Layer Depth and Subsurface Layer Thickness Acronyms and Descriptions

Labels	Defined	Description
	Surface Layer Depths	
IPLD	iso-pycnal layer depth	Estimated by variable density threshold based on 0.2°C temperature change [*Kara et al.*, 2000a]
ITLD	iso-thermal layer depth	Estimated by 0.2°C temperature threshold
IHLD	iso-haline layer depth	Estimated by variable salinity threshold based on 0.2°C temperature change (see section 4.1)
MLD	mixed layer depth	Minimum of IPLD, ITLD, and IHLD
	Subsurface Layer Thicknesses	
ITGLT	isothermal density gradient layer thickness	ITLD-IPLD
IHGLT	isohaline density gradient layer thickness	IHLD-IPLD
CLT	compensation layer thickness	IPLD-MLD
TLT	transition layer thickness	Distance between the MLD and the last half-maximum buoyancy frequency (section 3)
	Dimensionless Index	
CI	T versus S Control Index	(IHLD-ITLD)/(ITLD+IHLD), Positive for T and negative for S control of the MLD (section 5)

[21] There are several methods for estimating the IPLD from in situ profile observations. The most widely used method is to compute the depth where potential density deviates from a near surface value by a variable threshold [*Kara et al.*, 2000a; *de Boyer Montégut et al.*, 2004]. Another method is based on the curvature of density with depth and has become more popular since *Lorbacher et al.* [2006] [*Helber et al.*, 2008; *Kara et al.*, 2010]. Recently, a hybrid approach by *Holte and Talley* [2009] implements both threshold and gradient calculations to assemble a suite of physical features from which to select an appropriate MLD. For the present analysis we have chosen the threshold methodology [*Kara et al.*, 2000a] for its simplicity and because it has been proven effective for global application.

[22] The reference values of potential density, potential temperature, and salinity for the layer depth calculations are taken from the reference depth, which is the shallowest in situ observation level in the depth range from 3 to 12 m. The layer depths are defined as the shallowest depth below the reference where the profile deviates from the reference by more than the threshold magnitude (either a positive or negative deviation). The layer depth is the linearly interpolated location of the threshold value. The thresholds are based on a 0.2°C offset, at the lower end of generally accepted values for estimating MLD [*de Boyer Montégut et al.*, 2004], which sets a relatively low tolerance for mixed layer property variability. ITLD directly uses a 0.2°C threshold, while for IPLD the threshold is the increase in density associated with a 0.2°C decrease in potential temperature at the reference salinity and depth. The IHLD threshold is the increase in salinity associated with a density increase equal to the IPLD threshold at constant reference temperature and depth. We calculate the IHLD threshold by increasing the salinity by 0.01 increments until the density threshold is met or exceeded. The surface layer depth labels with descriptions are listed in Table 1.

[23] A single profile may return different values for these three layer depths even though all of the depths are calculated using the same observed near-surface T and S reference depth and all use thresholds associated with a 0.2°C offset. For this paper, MLD is defined to be the shallowest depth among IPLD, ITLD, and IHLD.

4.2. Isothermal and Isohaline Density Gradient and Compensated Layers

[24] The mixed layer depth MLD is the shallowest depth where a profile's T, S, or density sufficiently deviates to indicate a beginning stratification. When the layer depth definitions are based on a shared threshold, the relative differences among IPLD, ITLD, and IHLD indicate the nature of the initial stratification below the mixed layer. We define the distance between the ITLD and the IPLD as the isothermal density gradient layer thickness (ITGLT) given by ITLD-IPLD and the isohaline density gradient layer thickness (IHGLT) given by IHLD-IPLD. The ITGLT (ITLD-IPLD) is similar to the "barrier" layer, which exists when IPLD is shallower than the surface isothermal layer depth defined by a threshold decrease in temperature from a near surface value [e.g., *Sprintall and Tomczak*, 1992]. Following *Kara et al.* [2000a], the ITLD in the present analysis is defined by an increase or decrease deviation from the near surface reference value, which in this case is 0.2°C. For this reason the ITGLT is not exactly the same as the "barrier" layer as defined in the scientific literature [e.g., *Cronin and McPhaden*, 2002]. In the case of a temperature inversion beneath the MLD, the ITGLT will represent the depth of the "barrier" layer minus the depth of the inversion below the MLD [*de Boyer Montégut et al.*, 2007], if one exists. Consistent for the purposes of the present article, the ITGLT represents the depth range over which temperature is relatively uniform while the salinity gradient results in a substantial density change. When ITGLT is greater than zero, salinity is controlling the location of the MLD. Conversely, the IHGLT represents the depth range over which salinity is relatively uniform while the temperature gradient results in a substantial density change. When IHGLT is greater than zero, temperature is controlling the location of the MLD.

[25] The histograms shown in Figure 3 indicate that the ITGLT and IHGLT are skewed toward the positive because compensated layers are much less common than gradient layers. Also, IHGLT tends to be greater than the ITGLT since temperature is the primary controlling factor of MLD. This occurs because a 0.2°C temperature threshold results in a density change that is larger than the density change

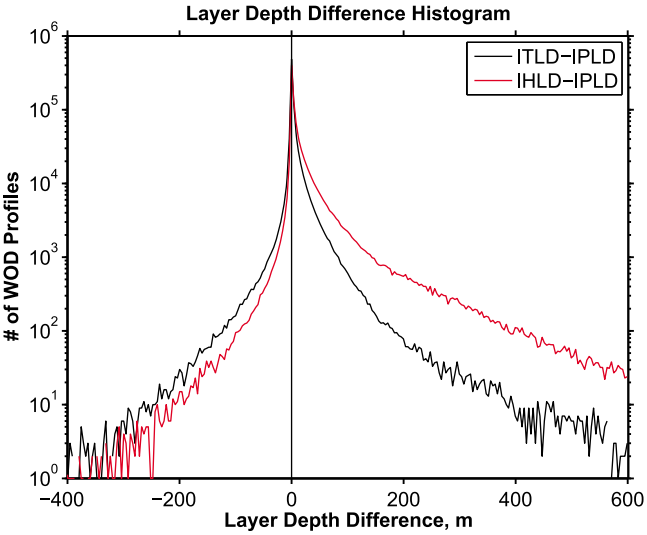

Figure 3. Histograms of the ITGLT (black line) and IHGLT (red line). Negative differences correspond to profiles where density compensation results in the IPLD being deeper than the ITLD or the IHLD.

caused by typical upper ocean salinity changes. Profiles where IPLD is deeper than both ITLD and IHLD (counted on the left side of Figure 3), are said to have a compensated layer because, below the MLD, gradients in temperature are compensated by gradients in salinity to maintain a uniform density down to the IPLD. Compensated layer thickness (CLT) is equivalent to the difference IPLD-MLD and is therefore the difference between our definition and the traditional definition of MLD. Names and definitions for these intermediate layers and their thicknesses are recorded in Table 1.

[26] A substantial amount of research has been conducted using the IPLD as the mixed layer depth [e.g., *Kara et al.*, 2000a; *de Boyer Montégut et al.*, 2004]. Traditionally, differences between the ITLD and the IPLD are discussed as barrier and compensated layer depths [e.g., *Kara et al.*, 2000b; *de Boyer Montégut et al.*, 2007; *Liu et al.*, 2009; *Mignot et al.*, 2009]. Typically, the IHLD has only received attention in regional studies [e.g., *Huyer et al.*, 2007]. The global statistics of IHLD are described in the present article.

[27] Considering the global high-resolution data set of layer depths, the IHLD, ITLD, and IPLD have quite different histograms (Figure 4). Using numbers from Figure 4, we find that 64% of MLDs from the high-resolution profiles are determined by the IPLD. In these profiles, IPLD is less than both ITLD and IHLD, which indicates that both temperature and salinity contributed to the density change at the base of the mixed layer. It is important to note that in many cases the difference among IPLD, ITLD, and IHLD are slight. This approach for classifying the temperature versus salinity control of the MLD does not differentiate between small and large differences between IPLD, ITLD, and IHLD. Nevertheless, in 25% of the data, ITLD was the shallowest layer depth, indicating that temperature gradient determined the MLD. In the remaining 11% of the data, IHLD was the shallowest layer depth. We investigate a potentially more meaningful measure of MLD determining factors in section 6.

4.3. The Transition Layer Thickness

[28] Ocean properties begin to vary with depth in the transition layer below the vertically uniform mixed layer. To estimate the transition layer thickness (TLT), we examine the observed vertical structure of squared buoyancy frequency (N^2). The calculation requires estimates of the background, maximum, and half-maximum N^2. While *Johnston and Rudnick* [2009] offer an alternative approach to compute the transition layer from observations including N^2 and velocity shear, velocity shear is unavailable for the global ocean data set used in this study.

[29] In this study we estimate TLT as the distance between the MLD and the deepest N^2 value that is equal to half of the maximum N^2 that occurs in the profile (hereafter N^2 half-maximum). To compute the N^2 half-maximum requires first determining the maximum N^2 and the background N^2 values of the profile. The background N^2 is determined by averaging from the reference depth to the MLD while the maximum N^2 is the largest value found in the profile. The N^2 half-maximum is then given by 1/2(maximum N^2 - background N^2).

[30] Examination of the data show that the magnitude and location of the maximum N^2 is subject to biases in low resolution profiles, with the high probability that a low resolution profile will miss the location and magnitude of the N^2 maximum. The reason is that a typical buoyancy frequency profile has local maxima at several depths (Figure 5d). For this reason, the location of the estimated N^2 maximum is not used directly to determine the TLT. We have found that the two most robust depth indicators in low resolution profiles are the MLD and the last half-maximum

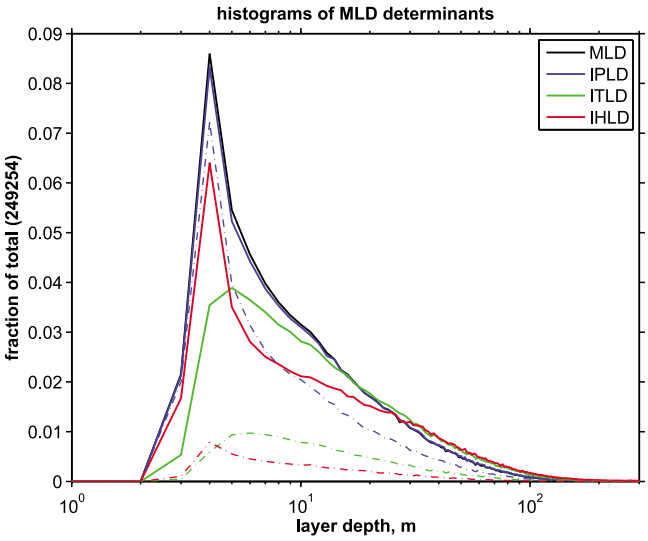

Figure 4. Histograms of MLD, IPLD, ITLD, and IHLD from the high-resolution data set (see section 2). Solid lines represent the total numbers computed from all profiles and are color coded as defined in the legend. Dash-dotted lines have the same color code as the solid lines and are histograms of layer depth restricted for only cases where IPLD, ITLD, or IHLD are the shallowest and therefore determine the MLD. The sum of the dash-dotted lines equals the solid black line, and 11, 25, and 64 percent of the MLD are determined by IHLD, ITLD, and IPLD, respectively.

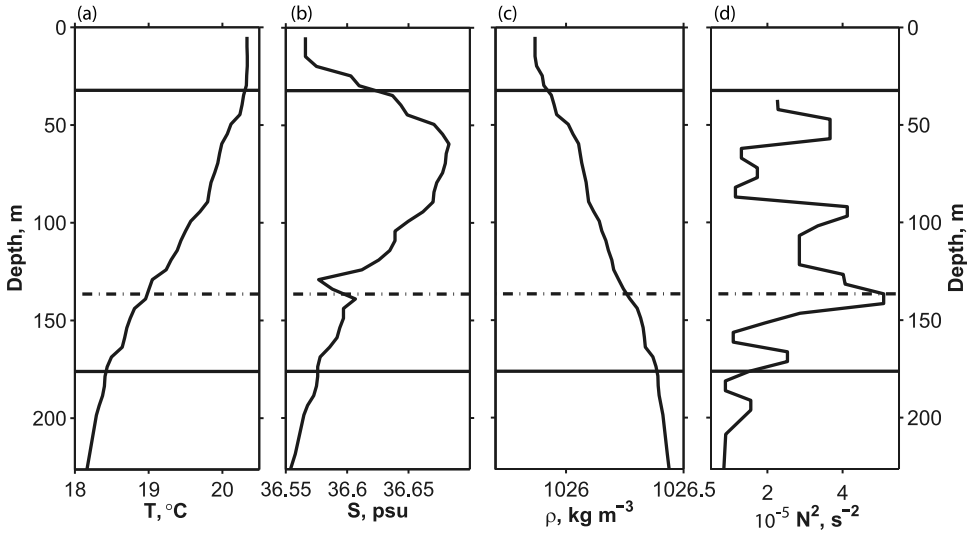

Figure 5. Example profiles of (a) temperature, (b) salinity, (c) potential density, and (d) buoyancy frequency from the North Atlantic. In each plot, the upper solid horizontal lines are at the MLD and the lower solid horizontal lines are at the last half-maximum buoyancy frequency. The dash-dotted line in each plot is at the depth of the buoyancy frequency maximum as computed from this Argo profile.

N^2 that occurs below both the MLD and the N^2 maximum. For the example profile in Figure 5, the MLD is 32 m and the half-maximum N^2 is 2.5×10^{-5} s^{-2}. The last N^2 local maximum that is greater than the half-maximum N^2 is located at 171 m. The bottom of the TLT is taken as the next buoyancy frequency value smaller than the half-maximum N^2, which is 1.5×10^{-5} s^{-2} and located at 176 m. The TLT for the profile in Figure 5 is therefore 144 m.

[31] The TLT identified using this approach is associated with larger scale processes than those studied by *Johnston and Rudnick* [2009]. With 10 m vertical resolution, it is not possible to compute a transition layer associated with small scale processes. Instead, the TLT used in this study represents the result of variability occurring on seasonal and longer time scales that may encompass the entire thermocline thickness.

4.4. Resolution

[32] Estimates of MLD are inherently vertical resolution dependent, and this must be addressed because we are using profiles with different vertical resolutions. When considering the vertical resolution relevant for ocean general circulation modeling [e.g., *Barron et al.*, 2006], Argo profiles are relatively representative. Even regional modeling studies tend to have resolution inadequate for resolving the transition layer as defined by *Johnston and Rudnick* [2009]. A goal of the present work is to perform an analysis that is consistently representative of one vertical resolution. Our goal is to provide a consistent treatment of the data to reduce biases from data with different sample spacing.

[33] Estimating MLD and TLT from low resolution Argo float profiles generally gives larger values than relatively high-resolution (~1 m) CTD profiles. To demonstrate this fact, we have taken all the CTD profiles that have resolution finer than 3 m and then subsampled and interpolated them at lower resolutions with depth level spacing of 2, 4, 6, 8, and 10 m. The raw profiles and each of the subsampled profiles are then used to estimate MLD and TLT (Figure 6). The statistical mode of MLD and TLT tends to increase with the depth sample spacing as shown in Table 2. Biases clearly occur for MLD and TLT smaller than about 20 m. In all cases but one, MLD and TLT increase with increasing depth spacing. The TLT mode decreases with depth spacing only for the example with 10 m depth resolution. In a recent MLD climatology [*de Boyer Montégut et al.*, 2004], profiles of different resolutions have been mixed together. To provide more consistent sampling fidelity, the present approach ensures that all profiles either originated or are interpolated to depth levels similar to Argo profiling floats (see section 3).

4.5. Noise Sensitivity Estimates

[34] To gauge the error sensitivity of MLD and TLT estimates, we perform a perturbation error analysis that represents the sensitivity of the parameter to profile noise. White noise is added to both T and S profiles prior to computing MLD and TLT. The perturbations are random with a mean of zero and a standard deviation of 0.015°C for temperature and 0.03 psu for salinity. The perturbation values were chosen to be roughly half the estimated error levels in mixed layer temperature and mixed layer salinity as estimated by CTDs [*Ando and McPhaden*, 1997]. This procedure is repeated 100 times for each profile. The standard deviation of the 100 re-computed MLD and TLT provides an estimate of noise sensitivity. Results are shown relative to MLD and TLT standard deviation in section 6.

4.6. Gridding

[35] We compute new global monthly 1/4° gridded fields of the vertically uniform layer depths (MLD, ITLD, IHLD, IPLD) and the thickness fields for transition layer (TLT), density gradient layers (ITGLT,IHGLT), and compensated layer (CLT). The fields for months February, May, August, and November are described in section 6 and the rest of the months are available in the auxiliary material.[1] The gridding

[1] Auxiliary materials are available in the HTML. doi:10.1029/2011JC007382.

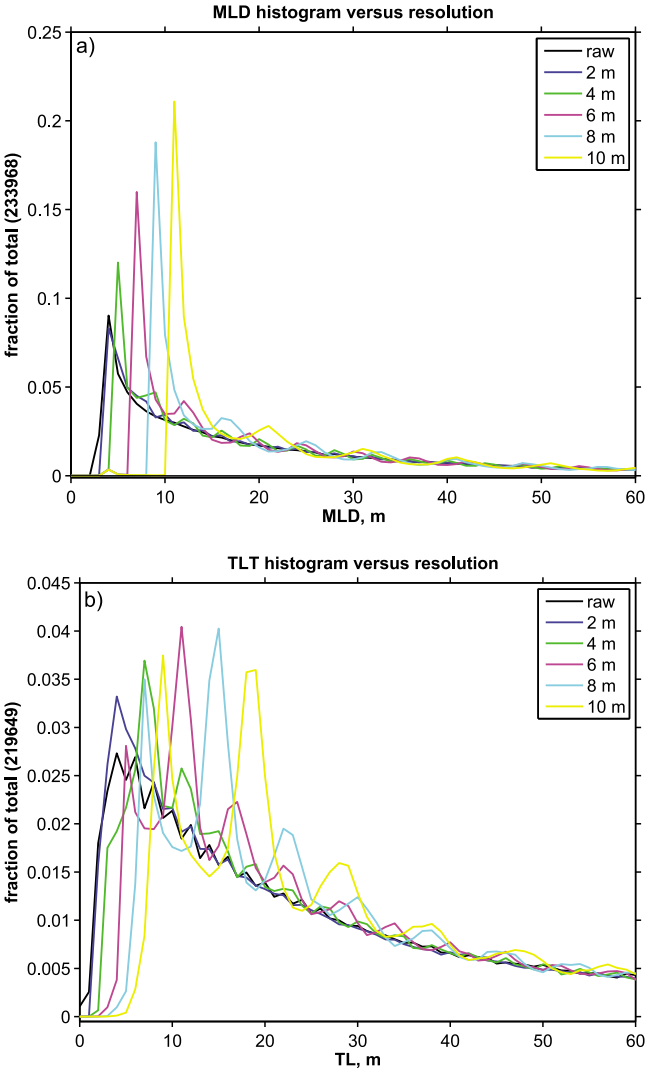

Figure 6. Histograms of (a) MLD and (b) TLT from 233,968 CTD profiles with <3 m depth sample spacing (most CTDs sampled at approximately 1m depth intervals). The black line represents the raw CTD histogram. The colored lines are from MLD estimates computed after the raw CTD profiles were sub-sampled at 2, 4, 6, 8, and 10 m depth spacing.

procedure for the climatology follows *Carnes et al.* [2010] and is based on a cost function designed to minimize the squared slope and data misfit to the gridded value,

$$J = \sum_m \sum_n \left\{ \left(\frac{T_{n+1,m} - T_{n,m}}{\Delta x_m / \Delta y} \right)^2 + \left(\frac{T_{n,m+1} - T_{n,m}}{1} \right)^2 + \sum_k \left(T_{m,n} - \theta_{m,n,k} \right)^2 \right\}. \quad (2)$$

[36] Here $T_{m,n}$ are the field solution being sought at grid points m, n that are not over land. On the regular 1/4° grid, the meridional distance between grid points Δy is constant, while Δx changes with latitude. Data for each month are selected to be within 45 days of the center of the month and are denoted $\theta_{m,n,k}$ in equation (2). Zero-gradient boundary conditions were applied at land boundaries to eliminate gridding over land and across land boundaries. The result of the minimization is a system of Poisson diffusion equations that we solve iteratively using the Gauss-Seidel method. Results are discussed in section 6. The main advantage of this solution is that it allows data values to diffuse around boundaries and into data gaps, providing a natural interpolator into regions with little data.

4.7. Standard Deviation

[37] The standard deviation is an important measure that clarifies the usefulness of the climatology estimates. The variance of MLD and TLT is computed as the squared anomalies of the observations from the monthly mean climatology. Using the techniques of section 4.6, the variances are gridded to a 1/4° regular grid. The square roots of the variances are the standard deviations, which are compared with the means and the noise sensitivity estimates and discussed in section 6.

5. Characteristic Profiles

[38] Figures 7a, 7b, 7c, 7d, and 7e show several examples of profiles from locations around the world that are structurally different and the results of different dynamical processes. In the North Atlantic during spring, temperature determines the MLD while the IHLD is much deeper (Figure 7a). When the ITLD is shallower than the IHLD, mixed layer temperature changes are having the largest impact on the vertical density gradient. Since the profile is from April, springtime surface warming due to relatively small latent heat flux cooling [*Yu and Weller*, 2007] and increased solar heat flux that warms the surface water while leaving salinity unchanged. As a result, the density gradient at the base of the MLD is due to temperature.

[39] The IHGLT for the case in Figure 7a is 136 m, but exhibits a weak destabilizing vertical salinity gradient within the isohaline gradient layer that starts at 54 m and extends to 190 m depth. While there is a small gradient in salinity between 54 m and 190 m depths, its influence on density is less than that of temperature.

[40] The structure is opposite in the western equatorial Pacific warm pool (Figure 7b), where warm surface temperatures are subjected to heavy rainfall creating surface freshening during westerly wind bursts [e.g., *Wijesekera and Gregg*, 1996; *Feng et al.*, 2000; *Cronin and McPhaden*, 2002]. As a result, the salinity gradient at the base of a lens of fresh water determines the MLD and both temperature and salinity tend to increase density with depth below the ITLD. When the IHLD is shallower than the ITLD (ITGLT = 36 m), changes in mixed layer salinity exert the largest impact on the vertical density gradient. The profile in Figure 7b is also an example of a very thin compensated layer (CLT = 3 m), where the IPLD is slightly deeper than the IHLD due to a very slight temperature increase between

Table 2. The MLD and TLT Mode of 233,968 and 219,649 Profiles, Respectively, Versus Vertical Depth Level Spacing

	Depth Level Spacing					
	~1 m (raw)	2 m	4 m	6 m	8 m	10 m
MLD mode (m)	4	4	5	7	9	11
TLT mode (m)	4	4	7	11	15	9

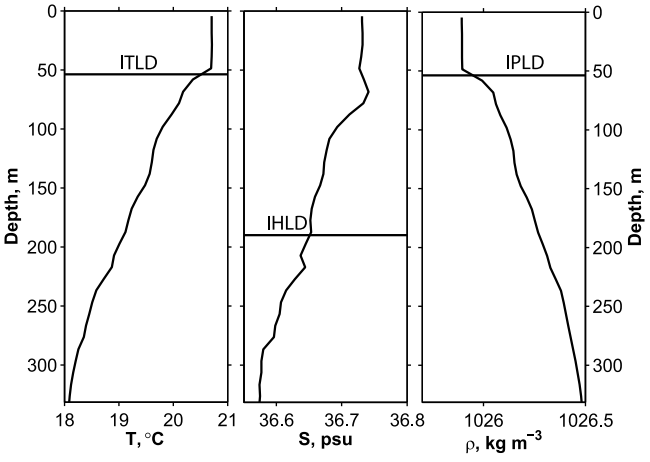

Figure 7a. Example profiles of (left) temperature, (middle) salinity, and (right) potential density from the North Atlantic Ocean (70°W, 35°N) in April. The layer depths of ITLD (54 m), IHLD (190 m), and IPLD (54 m) (from left to right) are represented by horizontal lines. The IHGLT is 136 m.

41 and 44 m depth. This thin compensated layer supports the methodology of making the MLD the shallowest of ITLD, IHLD, and IPLD.

[41] At higher latitudes in the Gulf of Alaska in February, precipitation is on a seasonal decline with a tendency for increasing salinity in the surface layer [*Ren and Riser*, 2009]. Surface salinity is driven primarily by precipitation [*Bingham et al.*, 2010], since latent and sensible heat fluxes are small in the Northeast Pacific Ocean [*Yu and Weller*, 2007]. For the example profile shown in Figure 7c, temperature increases with depth below the MLD. The sharp salinity gradient compensates for the temperature inversion. Salinity is the controlling gradient at the MLD because

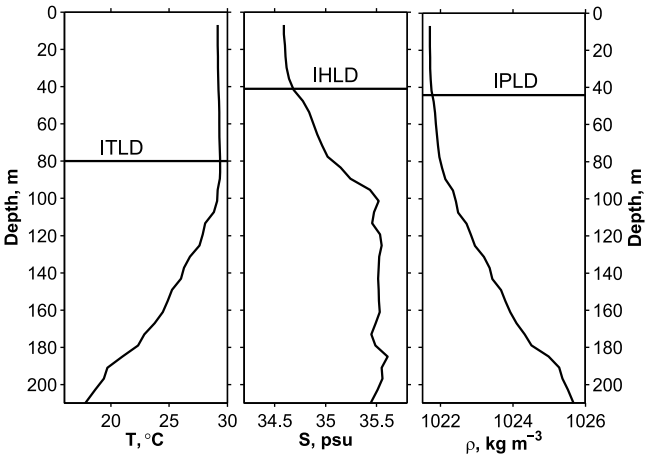

Figure 7b. Example profiles of (left) temperature, (middle) salinity, and (right) potential density the equatorial Pacific warm pool (156°E, 3°S) in April. The layer depths of ITLD (80 m), IHLD (41 m) and IPLD (44 m) (from left to right) are represented by horizontal lines. The ITGLT is 36 m and the CLT is 3 m.

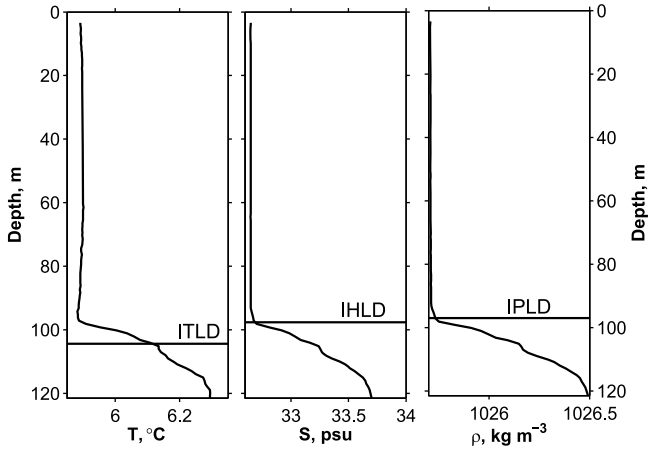

Figure 7c. Example profiles of (left) temperature, (middle) salinity, and (right) potential density from the Gulf of Alaska (142°W, 50°N) in February. The layer depths of ITLD (104 m), IHLD (98 m), and IPLD (97 m) (from left to right) are represented by horizontal lines. The ITGLT is 7 m.

ITLD (104 m) is greater than the IHLD (98 m). While temperature also has a gradient, the temperature variation is very small and salinity makes a larger contribution to the density gradient.

[42] River outflow can have a measurable effect on the upper ocean, as shown in Figure 7d. The large freshwater outflow from the Ganges River produces a fresh surface layer and hence the IHLD is shallower than the ITLD [e.g., *Girishkumar et al.*, 2011]. Here, salinity is having the largest impact on the vertical density gradient at the base of the mixed layer, while the top of the thermocline is deeper.

[43] In the South Pacific under the Peru-Chile stratus cloud region [e.g., *Colbo and Weller*, 2007], vertical salinity gradients nearly compensate for temperature gradients, resulting in the ITLD and IHLD being nearly equal

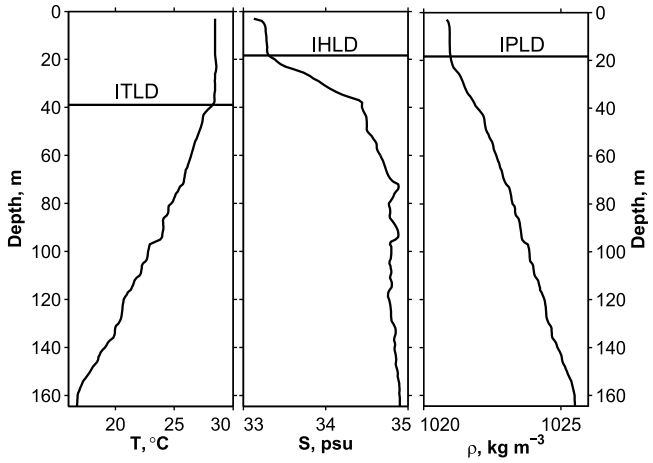

Figure 7d. Example profiles of (left) temperature, (middle) salinity, and (right) potential density from the Bay of Bengal (90°E, 15°N) in November. The layer depths of ITLD (39 m), IHLD (18 m), and IPLD (18 m) (from left to right) are represented by horizontal lines. The ITGLT is 21 m.

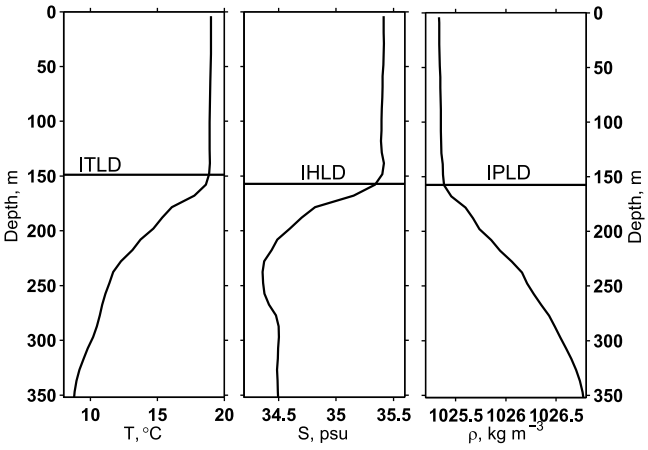

Figure 7e. Example profiles of (left) temperature, (middle) salinity, and (right) potential density from the South Pacific (90°W, 20°S) in July. The layer depths of ITLD (149 m), IHLD (157 m), and IPLD (157 m) (from left to right) are represented by horizontal lines. The CLT is 8 m.

(Figure 7e). Since ITLD is slightly shallower than IPLD, there is a thin CLT of 8 m. The ocean beneath the Peru-Chile stratus clouds is complex and neither temperature nor salinity dominates the gradient at the MLD consistently. Generally, both temperature and salinity contribute to the vertical density gradient, since interactions of both temperature and salinity are required for accurate modeling the southeast Pacific [*Toniazzo et al.*, 2010].

6. MLD Climatology

[44] Monthly fields of MLD are computed using the gridding methods described in section 4.6 and are shown for the months of February, May, August, and November (Figures 8 and 9). The months of February and August are the extremes of seasonal MLD, while May and November are transitional months when the rate of change of MLD is largest at mid latitudes. Also shown in Figures 8 and 9 are the standard deviation and noise sensitivity associated with MLD for the same months. Standard deviation fields are based on the gridded anomalies of each profile from the original gridded climatology and they characterize the observed MLD variability. The MLD noise sensitivity fields are the gridded standard deviation of 100 MLD estimates computed from each profile observation repeatedly given random temperature and salinity perturbations (see section 4.5). The magnitude of the MLD noise sensitivity is roughly half as large as MLD standard deviation (Figures 8 and 9) with some exceptions.

[45] In February, in the North Atlantic at approximately 50°N, the MLD is very deep due to strong surface cooling by latent and sensible heat flux [e.g., *Yu and Weller*, 2007], creating nearly uniform temperature with depth at high latitudes in winter (Figure 8a). The MLD estimate when temperature and salinity are uniform down to large depths in winter at high latitudes, does not necessarily mean that active mixing is occurring continuously down to that depth. In contrast, summer hemisphere MLD estimates such as those at mid southern latitudes (also in February, Figure 8a) are generally less than 40 m and are likely to have strong gradients at the base of the mixed layer, constraining mixing near the surface. In the southern latitudes in February, the latent and particularly the sensible heat flux tendency to cool the ocean is substantially reduced compared to the northern hemisphere [*Yu and Weller*, 2007].

[46] By May, the northern hemisphere MLD has shoaled and the southern hemisphere MLD has begun to deepen (Figure 8b). In August, the MLD is at its shallowest point in the northern hemisphere and the deepest point in the southern hemisphere (Figure 9a). November is a transition month where MLD is deepening in the northern hemisphere and shoaling in the southern hemisphere (Figure 9b).

[47] Mixed layer depth variability for a given region is represented in Figures 8c, 8d, 9c, and 9d. The largest standard deviation occurs in the winter hemisphere at high latitudes (Figures 8c and 9c). At high latitudes when the surface is nearly as cold as the deep ocean, MLD estimates become deep because temperature is isothermal from the surface to the deep ocean. If the salinity variability is also small, MLD estimates will reach the bottom of the observation profile or the ocean bottom itself. If a slight warming occurs, the estimate of the MLD that was previously at the bottom will jump to near the surface as warming occurs at the surface. This is the reason for large standard deviations at high latitudes in winter. In the transitional months of May and November, the MLD standard deviation is more geographically uniform and relatively small (Figures 8d and 9d) compared to winter time MLD deviations.

[48] Mixed layer depth noise sensitivity estimates are largest in the geographical transition regions between the tropics and high latitudes (Figures 8e and 9e). Large noise sensitivity does not coincide with large standard deviation. For example, in February, the MLD noise sensitivity estimate is large at approximately 30°N in the Atlantic and the Pacific (Figure 8e). The peak standard deviation tends to occur farther north (Figure 8c) [e.g., *Carton et al.*, 2008]. In the southern hemisphere, large noise sensitivity occurs at approximately 35°S (Figure 9e). As we will see in the next section, MLD sensitivity is largest in regions where transition layer temperature and salinity gradients both contribute to the MLD. Large noise sensitivity estimates indicate that small perturbations in T or S will change the depth of the MLD substantially.

[49] In Figure 10, ITGLT and IHGLT are shown for months of February, May, August and November. A larger than zero ITGLT means that vertical temperature gradients are too small near the surface to identify the MLD. For the IHGLT the opposite is true, vertical salinity gradients are too small near the surface to identify the MLD. The IHGLT is much larger than the ITGLT over most of the ocean because vertical temperature gradients are the primary determining factor for the MLD.

[50] The seasonal patterns for isothermal and isohaline gradient layers complement each other because when IHGLT is large ITGLT is small and visa versa. For example, large ITGLT exist in the North Pacific north of ~40°N [*Kara et al.*, 2000b] in February while the IHGLT is near zero. Salinity gradients dominate in the upper ocean in the North Pacific due to large precipitation and low latent heat flux, as discussed regarding the profile in Figure 7c. Large ITGLT also tend to occur in the tropical warm pool areas, where their impact on climate is considered to be large [e.g.,

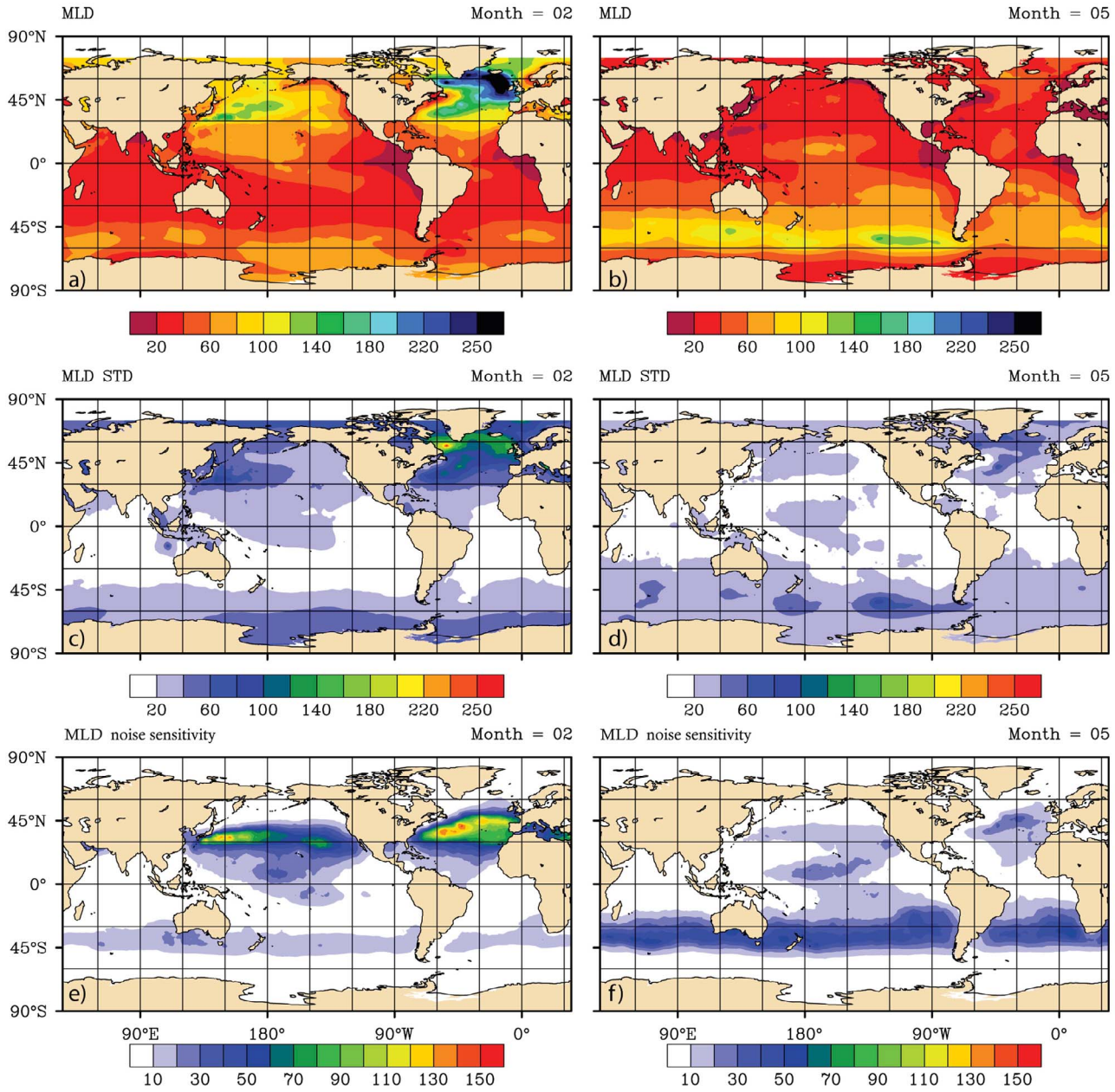

Figure 8. The global 1/4° gridded MLD for (a) February and (b) May along with the associated (c, d) standard deviation and (e, f) noise sensitivity. Color coded values are in m with a 20 m contour interval for Figures 8a–8d and 10 m contour interval for Figures 8e and 8f. The color map range is 100 m smaller in Figures 8e and 8f.

Mignot et al., 2007]. While estimates of MLD standard deviation are small in the tropics (Figures 8c, 8d, 9c, and 9d), variability of barrier layers is large [*Mignot et al.*, 2009]. The latter occurs because the formation of barrier layers is episodic with the variability of local rainfall patterns.

[51] Large IHGLT occurs much more frequently at mid latitudes and along the equatorward side of western boundary current regions (e.g., see Figure 7a). There is also a very large IHGLT region associated with the Antarctic circumpolar Current particularly in austral summer. The IHGLT is large wherever temperature gradients dominate the control of the MLD and salinity vertical variably is small. In the regions near western boundary currents there is large latent and sensible heat flux out of the ocean [*Yu and Weller*, 2007], which influences temperature more strongly than salinity. As a result, temperature is the dominant gradient at the MLD and IHGLT is large. This also occurs beneath the large latent and sensible heat flux in the region of the Antarctic circumpolar Current. To our knowledge, the isohaline gradient layer has not been a subject of previous study on a global scale.

7. Density Compensation and MLD Control

[52] The compensated layer thickness, CLT, is computed as IPLD-MLD and represents the difference between our

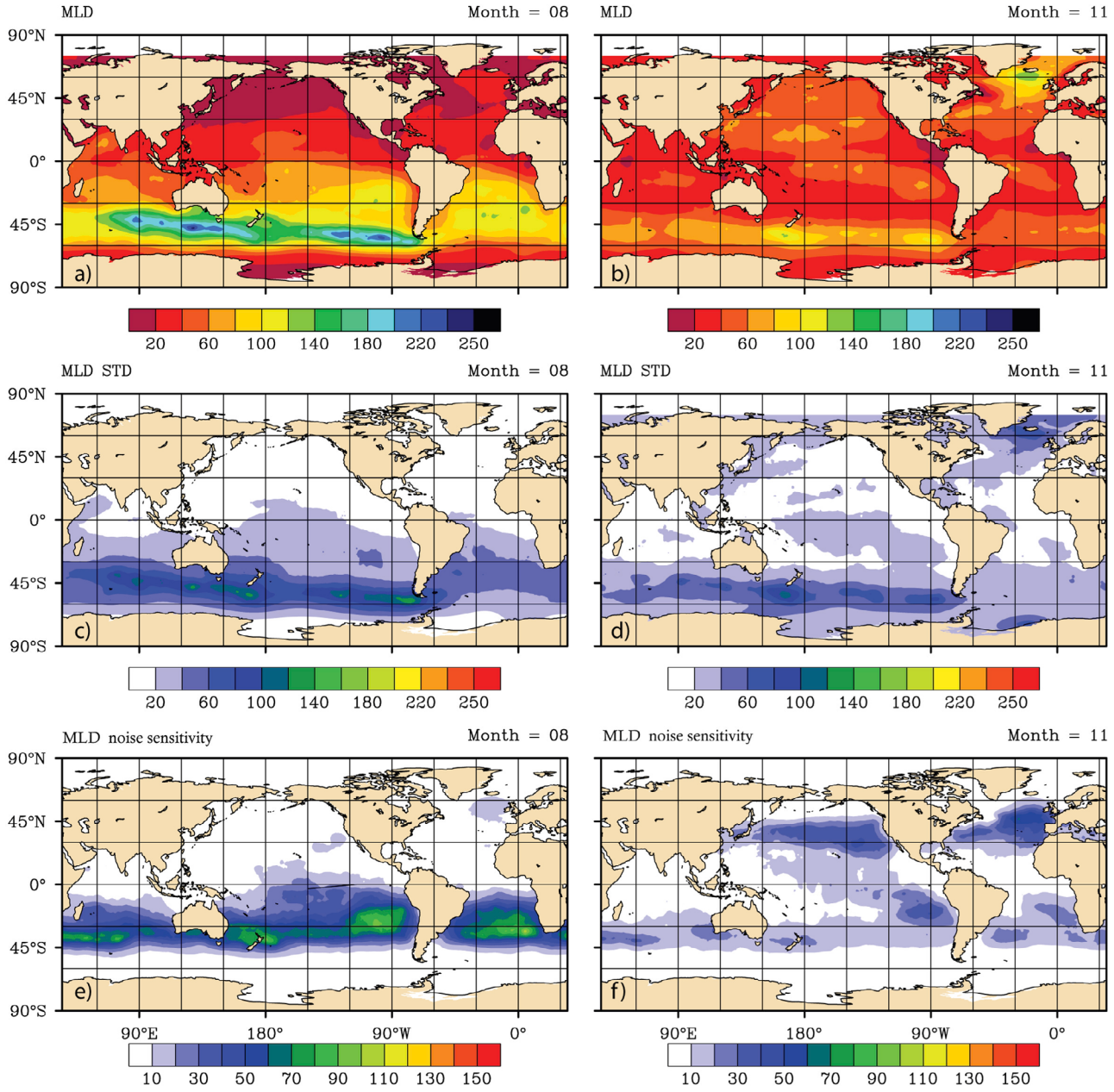

Figure 9. Same as in Figure 8 but for August and November.

definition and the traditional definition of MLD. Over much of the ocean CLT is much smaller than the ITGLT and IHGLT. It can be large, particularly in the North Atlantic Ocean during winter (Figure 11). The compensated layer is also thick in a large region south of Australia in August. In cases where CLT is large, both temperature and salinity tend to be uniform over a broad depth range.

[53] To understand the relationship between barrier and compensated layers, we have selected three regions of the ocean to examine the time series over the seasonal cycle. In the South Pacific region below the persistent Chile-Peru stratus cloud cover [e.g., *Colbo and Weller*, 2007] at 20.5°S, 89.5°W (Figure 12), we have relatively large CLT (Figure 11) combined with thin barrier layers (Figure 10). As a measure of T versus S control of the mixed layer depth, we define a T versus S control index, CI, given by:

$$CI = \frac{(IHLD - ITLD)}{(ITLD + IHLD)}. \quad (3)$$

[54] For positive values of CI, the IHLD is deeper than the ITLD indicating that temperature determines the MLD. For negative values the opposite is true, and salinity determines the MLD.

[55] In the South Pacific, temperature determines the MLD most strongly in the austral summer months of November through February (Figure 12b). During April through September, CI is close to zero indicating that the

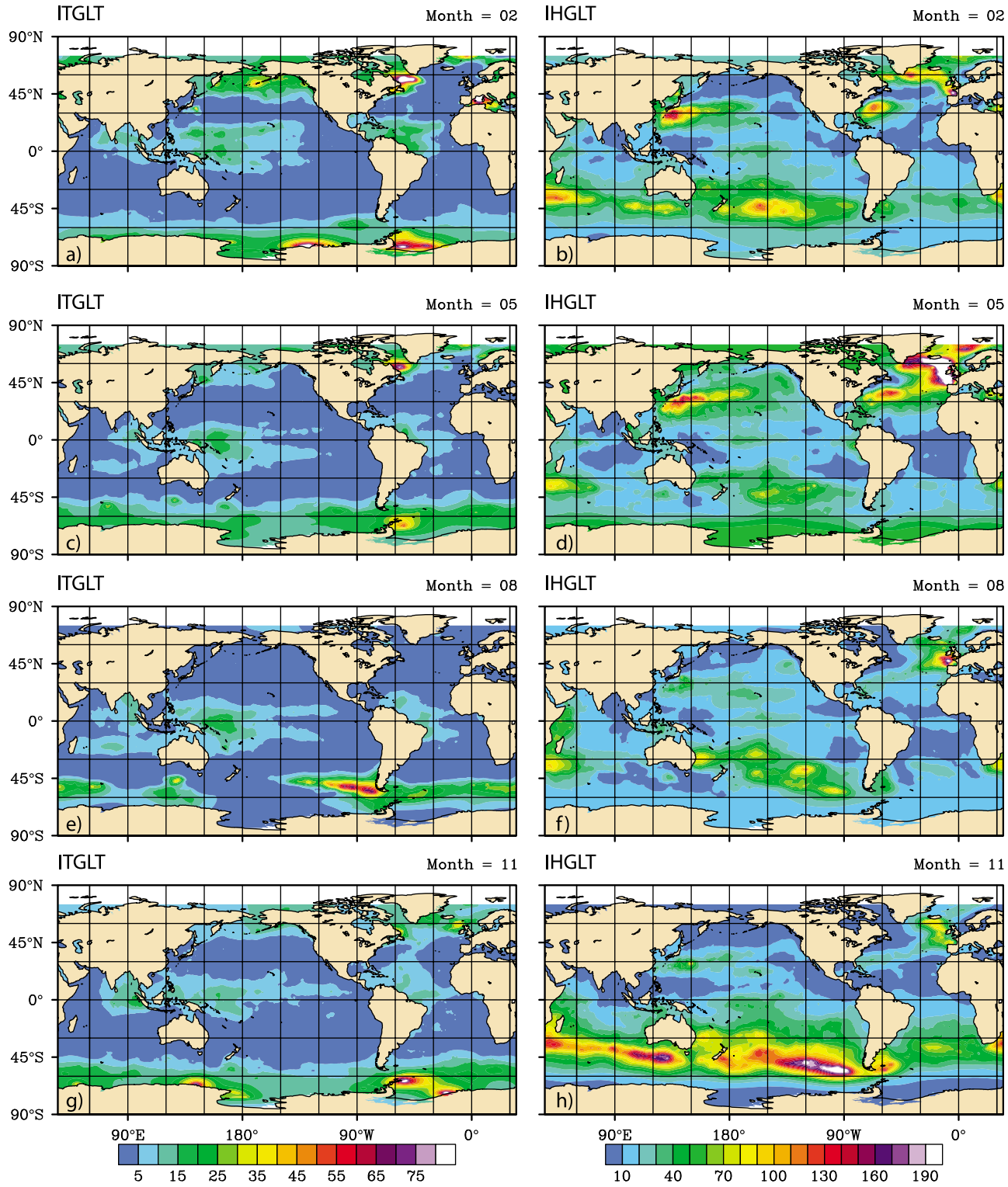

Figure 10. The global 1/4° gridded (a, c, e, g) ITGLT and (b, d, f, h) IHGLT for February (Figures 10a and 10b), May (Figures 10c and 10d), August (Figures 10e and 10f), and November (Figures 10g and 10h). Color coded units are in m with a contour interval of 5 m for ITGLT and 10 m for IHGLT.

IHLD and ITLD are close. While temperature determines the MLD most of the time, salinity at this location has a substantial role and ITGLT is very thin. Both temperature and salinity contribute to upper ocean variability.

[56] In the Gulf of Alaska, the variability is different. Temperature and salinity seasonally alternate control over the MLD (Figure 13), and temperature and salinity do not create a compensated layer. In the summer, when warm near-surface waters exists during the seasonal minimum in

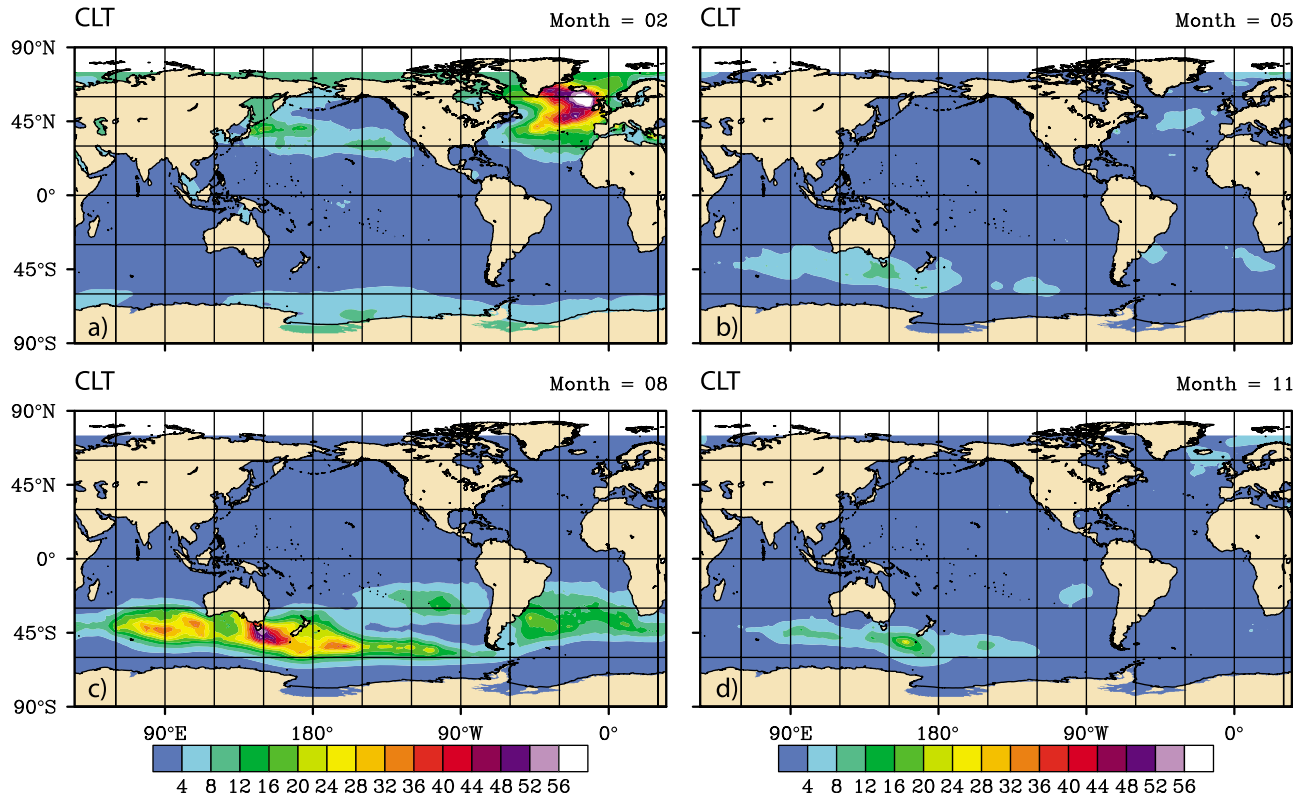

Figure 11. The global 1/4° gridded compensated layer thickness for the months of (a) February, (b) May, (c) August, and (d) November. The color coded units are m with a contour interval of 4 m.

precipitation [*Ren and Riser*, 2009], T controls the MLD as it becomes cooler with depth. During the winter, temperature is nearly isothermal all the way to the bottom and salinity controls the MLD during a season when precipitation is greater. Since surface heat fluxes are relatively small in the Gulf of Alaska, the salinity conservation equation (equation (1b)) must balance the large fluctuations of $E - P$. Salinity tendency, advection, and turbulent flux of salinity at the MLD must have a major role in the MLD regulation.

[57] At a midlatitude location near the Gulf Stream in the North Atlantic (29.8°N 75.5°W), T maintains control throughout the year (Figure 14). The IHLD is very deep, indicating that salinity in the upper ocean does not vary enough to alter the MLD. Compensation of T and S remains small. In this region, latent and sensible heat flux is large [*Yu and Weller*, 2007] and precipitation is relatively low [*Adler et al.*, 2003], suggesting that the mixed layer is governed by the temperature conservation equation (equation (1a)), while the influence of equation (1b) is negligible.

[58] For the months of February, May, August, and November, the CI gridded to 1/4° is shown in Figure 15. Positive values indicate that temperature has the controlling gradient at the MLD and negative values indicate that salinity has the controlling gradient at the MLD. Large parts of the ocean are positive (red) in the subtropics, where temperature controls the MLD. Salinity controls the MLD near large river outflows, in parts of the tropics, and at high latitudes. The white areas are where temperature and salinity are in opposition and have nearly equal contribution to the depth of the mixed layer.

[59] The temperature and salinity control index (CI) sorts the ocean into three regimes that each tend to have a distinct type of mixed layer. The first type is where vertical gradient of temperature in the transition layer determines the MLD. When temperature is the controlling factor, CI is positive and the processes at work in the mixed layer tend to modify temperature more than salinity, in terms of density. Temperature is the controlling gradient at the base of the mixed layer (where $CI > 0.05$) for 63% of all ocean data points from the 12 monthly means. Regions with large positive CI tend to occur where surface heat fluxes dominate the conservation equations (1a) and (1b). The positive regions of Figure 15 tend to be where latent and sensible heat flux are large and cooling the ocean [*Yu and Weller*, 2007].

[60] The second condition occurs when salinity is the controlling factor (the classic barrier layer); CI is negative and the processes at work in the mixed layer tend to modify salinity more than temperature, in terms of density. Salinity is the controlling gradient at the base of the mixed layer (where $CI < -0.05$) for 14% of all ocean data points from the 12 monthly means. Regions with large negative CI tend to occur where precipitation is large and surface heat fluxes are small. The negative regions of Figure 15 tend to be where precipitation is large, particularly in the tropics [*Adler et al.*, 2003]. One region where precipitation is not large but CI is negative is in the Bay of Bengal, where outflow from the Ganges River is large. The Bay of Bengal is known to have barrier layer formation due to river input [e.g., *Girishkumar et al.*, 2011].

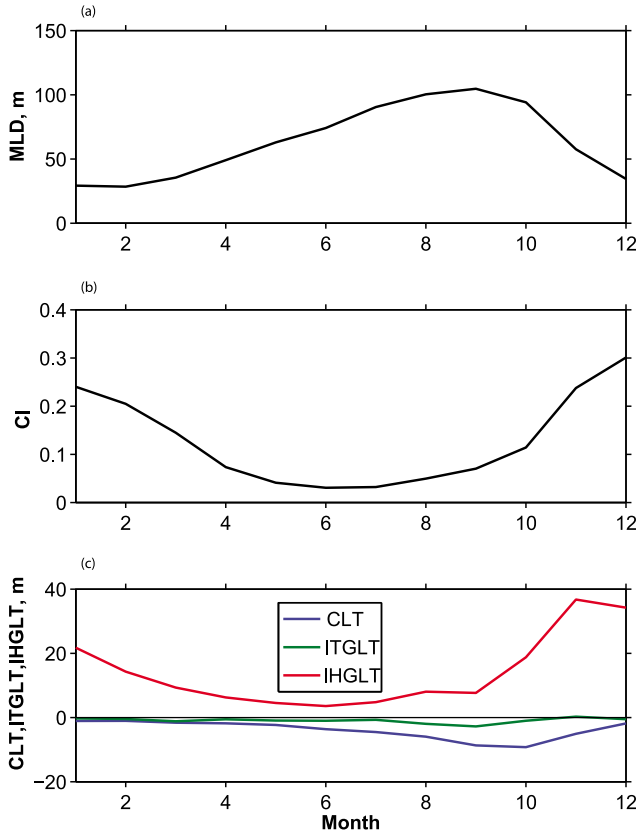

Figure 12. Time series from the 1/4° gridded climatology of (a) MLD; (b) CI; and (c) ITGLT, IHGLT, and CLT at a location in the stratus deck region of the South Pacific (20.5S, 89.5W).

[61] The third condition occurs when both the temperature and salinity gradients at the bottom of the mixed layer contribute to control of the MLD. In this case, processes controlling temperature and salinity are both at work at the same time and with similar magnitude relative to density. Both temperature and salinity gradients contribute the MLD depth when $|Cl| \leq 0.05$; such conditions occur for 23% of all ocean data points from the 12 monthly means. An example of a region where CI is relatively small is found in the South Pacific beneath the persistent stratus cloud deck, where both temperature and salinity are important for modeling the dynamics accurately [*Zheng et al.*, 2010].

8. Transition Layer Thickness

[62] The thickness of the transition layer is problematic to determine, given the limited vertical resolution of the data, as discussed in sections 4.3 and 4.4. Nevertheless, estimates of TLT provide information regarding the properties of the ocean surface boundary layer below the MLD.

[63] In February, the TLT tends to be thick in the northern (winter) hemisphere and thin in the southern (summer) hemisphere (Figure 16a). Patterns are similar to those of MLD (Figure 8a) with the exception of the northeast Pacific, the tropics and the circumpolar current region. Since deep water is not formed in the North Pacific, deep water is warmer than the surface water in winter (Figure 7c). For this reason, the TLT is relatively thin in the northeast Pacific.

[64] In May, the patterns of MLD and TLT are nearly in opposition. In the North Pacific and Atlantic, the MLD shoals more quickly than the base of the TLT. Similarly, during the northern transition from summer to winter in November, MLD has already begun to deepen while the base of the TLT is still relatively shallow. This suggests that the seasonal cycle of TLT lags behind that of MLD.

9. Summary and Conclusions

[65] This research focuses on the gradients of temperature and salinity just below the mixed layer. With the mixed layer defined as vertically uniform in temperature, salinity, and density, then depths with vertical gradients in any of these properties are part of the transition layer. Examining the global variability of the transition layer gradients observed by in situ ocean profiles from floats and CTDs, we determine the relative contributions of temperature and salinity to the depth of the mixed layer (section 7, Figure 15). In 63% of the global ocean, based on all months, the MLD is determined by temperature gradients at the base of the mixed layer. Only 14% of the ocean has MLDs determined by salinity gradients. The remainder of the ocean, 23%, has gradients of temperature and salinity close to the same depth, both contributing to the MLD.

[66] Defining the MLD as the minimum of ITLD, IHLD, and IPLD (Table 1) makes the methodology more reliable than using IPLD as the MLD. Due to density compensation,

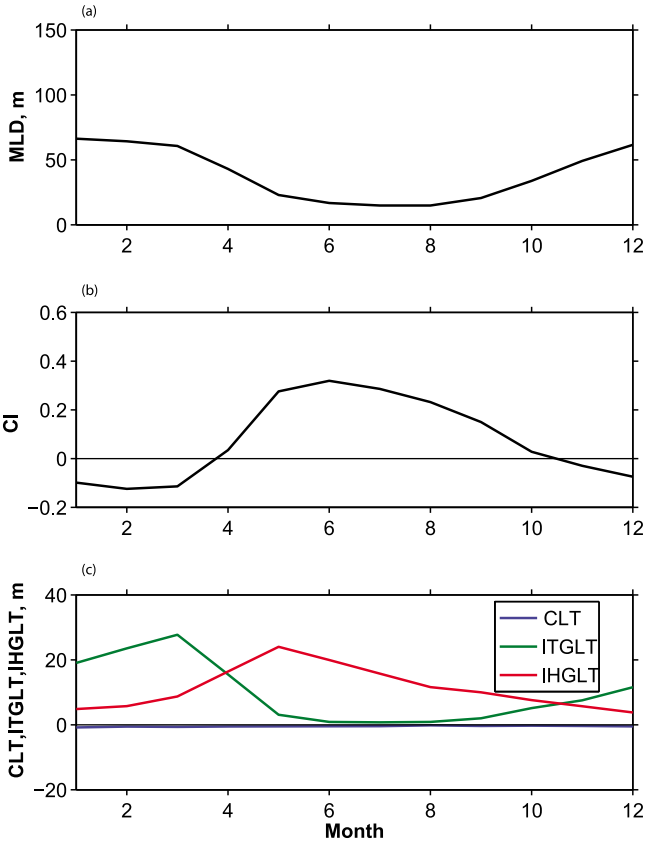

Figure 13. Time series from the 1/4° gridded climatology of (a) MLD; (b) CI; and (c) ITGLT, IHGLT, and CLT at a location in the Gulf of Alaska (54.75N, 145.25W).

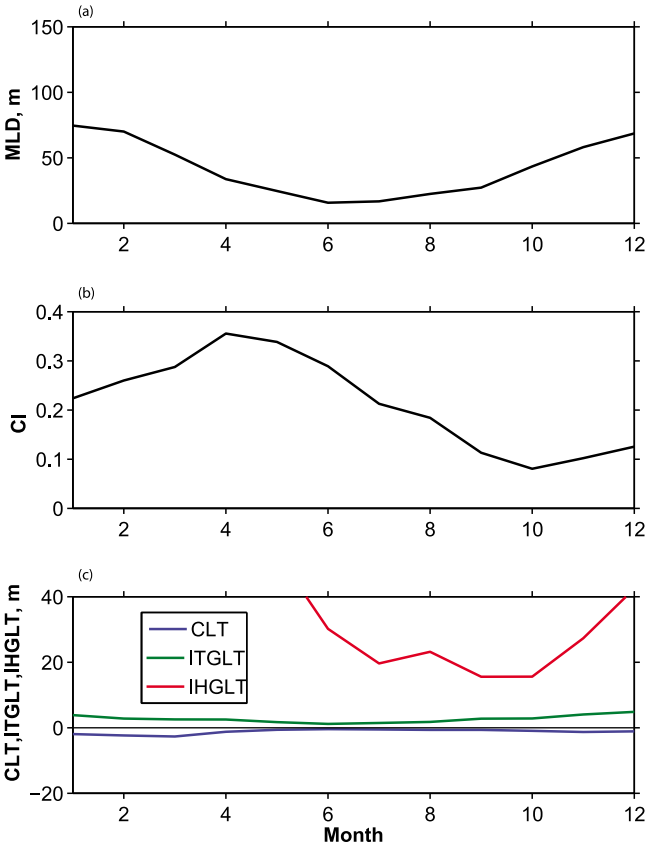

Figure 14. Time series from the 1/4° gridded climatology of (a) MLD; (b) CI; and (c) ITGLT, IHGLT, and CLT at a location in the North Atlantic (29.75N, 75.5W).

ITLD and IHLD become shallower than IPLD for 25% and 11% of all profiles, respectively. As a result, our definition of MLD differs from the traditional definition in 36% of all profiles. This approach is particularly useful at high latitude locations, where the temperature variability over the entire water column is very small (Figure 7c), and in barrier layer regions (Figures 7b and 7e). The methods described in this paper are recommended for applications requiring a reliable global measure of the MLD to represent the depth of vertically uniform surface ocean properties.

[67] A mixed layer depth determined by a sharp salinity gradient is different from a mixed layer depth determined by a sharp temperature gradient. When salinity determined the gradient at the bottom of a mixed layer, then mixing has a larger effect on salinity than temperature. In this case, the salinity conservation equation (1b) provides the more important mixed layer balance than the temperature conservation equation. The present analysis indicates that salinity tends to dominates the gradients at the MLD in regions where $E - P$ is large. Conversely, temperature dominates the gradients at the MLD where surface heat fluxes are large and the temperature conservation equation (1a) provides the more important mixed layer balance.

[68] The specific questions addressed in this article are:

[69] 1. Where in the global ocean during the annual cycle is the MLD determined by gradients of either temperature or salinity? In Figure 15, large areas of the subtropical ocean have $Cl > 0.1$, indicating the ITLD is substantially shallower than IHLD and the temperature gradients determine MLD. Salinity gradients dominate MLD where $Cl < 0.1$, i.e., in regions near large river outflows, in part of the tropics, and at high latitudes. During winter, control of temperature gradients is weakened at mid latitudes and salinity controls the MLD most strongly at high latitudes. Salinity control in the tropics, particularly in the warm pool regions, is persistent throughout the annual cycle.

[70] 2. Where in the global ocean during the annual cycle do transition layer gradients of temperature and salinity occur at the same depth? When the transition layer gradients of T and S occur near the same depth, IHLD is close to ITLD and $|Cl| < 0.1$. During winter, such conditions are found at midlatitudes surrounding subtropical gyres, but do not occur in gyre interiors (Figures 15a and 15c). In winter, ITLD and IHLD also coincide on the equatorward side of the polar front. In the tropics, low magnitude of CI occur north and south of the equator, but not on the equator. Temperature and salinity gradients are also found at similar depths beneath the Peru-Chile stratus cloud cover region nearly year-round.

[71] 3. What are some likely processes responsible for the temperature or salinity control of the MLD? To lowest order, the magnitude of $E - P$ versus Q_0 governs whether temperature or salinity is the controlling gradient at the MLD. There exists a general tendency for temperature controlled MLD where Q_0 is large and $E - P$ is small, and conversely salinity controlled MLD occurs where $E - P$ is large and Q_0 is small. More detailed analyses are required to quantify the relative influence of other processes such as advection, penetrative heat flux, and turbulent fluxes at the MLD.

[72] 4. Where in the global ocean during the annual cycle does large variability and noise sensitivity increase the uncertainty of the ocean MLD climatology? These distributions are shown in Figures 8 and 9. At high latitudes during winter, for example, the MLD becomes very deep because temperature becomes nearly uniform with depth. In the North Atlantic, Labrador Sea Water is formed episodically during deep convection events. As episodic warming events occur at the end of winter, MLD can vary over large depth ranges, creating a large MLD standard deviation. The climatological mean MLD computed from observations taken during a month with widely varying stratification may not be representative of an MLD that would actually occur. As a result, estimates of mean monthly MLD are more uncertain where the MLD standard deviation is large. In addition, regions of the ocean where MLD noise sensitivity is large indicate that small perturbations in temperature or salinity have a large influence on the estimates of MLD. Thus, the uncertainty of monthly MLD estimates is also larger in areas with large MLD noise sensitivity.

[73] 5. How does vertical resolution of in situ profile observations impact estimates of the MLD and transition layer thickness? The answer is that both MLD and TLT estimates tend to be deeper and thicker, respectively, when profile resolution is decreased. Since resolution has influence on the MLD estimates, mixing high and low resolution profiles together could artificially inflate barrier layer variance. For this reason, all estimates of MLD for the present study are computed after all observations are interpolated to the depth sampling of Argo profiling floats, which is approximately every 10 m.

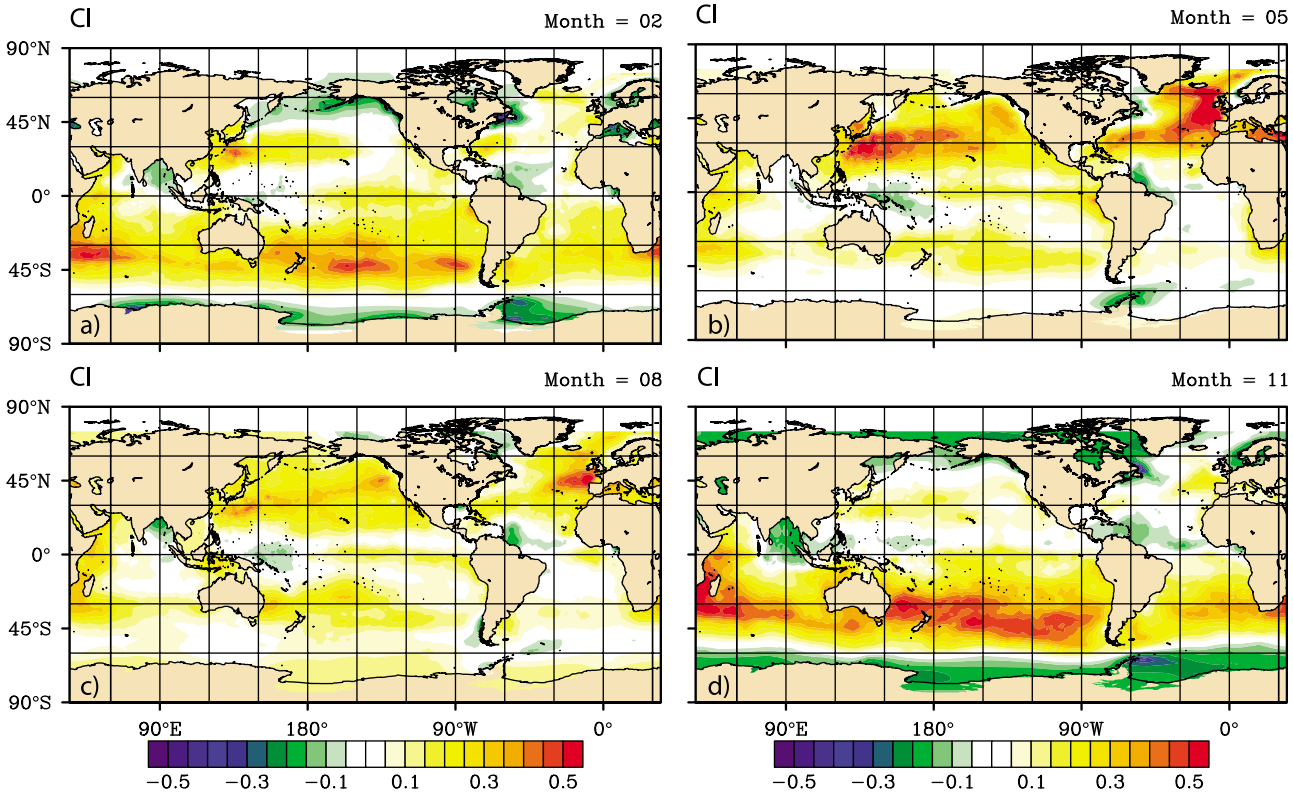

Figure 15. The 1/4° gridded temperature versus salinity control index for (a) February, (b) May, (c) August, and (d) November. The contour interval is 0.05 non-dimensional units.

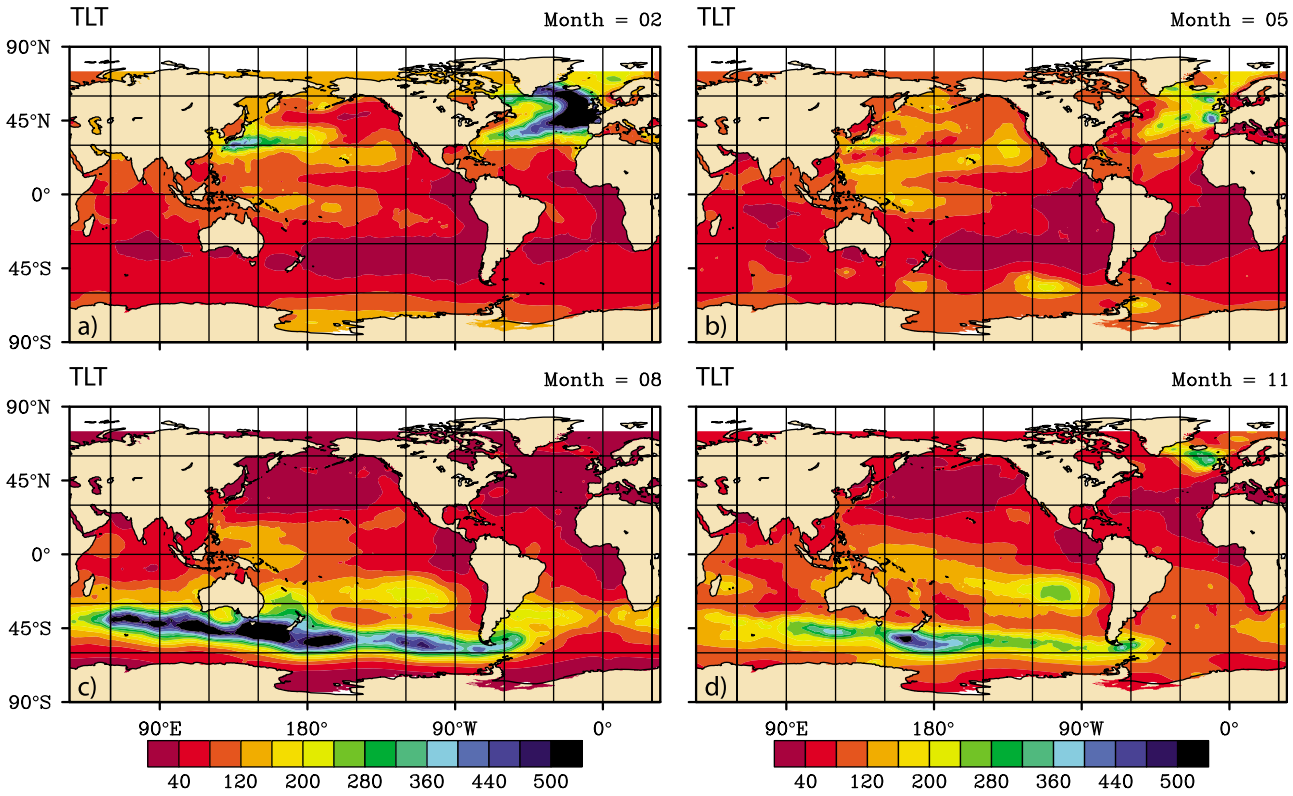

Figure 16. The 1/4° gridded transition layer thickness (TLT) estimates for (a) February, (b) May, (c) August, and (d) November. Color coded values are in m with a 40 m contour interval.

[74] For the first time, the isohaline layer depth has been considered globally, allowing us to characterize the vertical gradient of temperature versus salinity below the mixed layer. By considering both the temperature and salinity variability we have taken a more generalized approach to investigation of the global upper ocean vertical structure. With the advent of more abundant salinity observations from the Argo profiling float array, the details of temperature and salinity interactions can be investigated more thoroughly. Research on this topic has the potential to increase the capabilities of climate modeling in addition to operational global ocean forecasting through improved understanding of the influence of salinity and more capable salinity data assimilation methodologies.

[75] **Acknowledgments.** This research is funded by the Office of Naval Research under two Naval Research Laboratory projects. The first is the 6.1 program element 61153N The Impact of Spice on Ocean circulation. The second is the 6.2 program element 62435N Full Column Mixing for Numerical Ocean Models. The authors would like to thank three reviewers for helpful comments and J. Dastugue for help with figure graphics. With sadness, the authors report that A. Birol Kara passed away on 14 September 2009. Early work related to this publication was done by Kara and subsequent research has been inspired by his legacy. This paper is contribution NRL/JA/7320—11–0695 and has been approved for public release.

References

Adler, R. F., et al. (2003), The Version-2 Global Precipitation Climatology Project (GPCP) monthly precipitation analysis (1979–present), *J. Hydrometeorol.*, *4*, 1147–1167, doi:10.1175/1525-7541(2003)004<1147:TVGPCP>2.0.CO;2.

Ando, K., and M. J. McPhaden (1997), Variability of surface layer hydrography in the tropical Pacific Ocean, *J. Geophys. Res.*, *102*, 23,063–23,078, doi:10.1029/97JC01443.

Barron, C. N., A. B. Kara, P. J. Martin, R. C. Rhodes, and L. F. Smedstad (2006), Formulation, implementation and examination of vertical coordinate choices in the Global Navy Coastal Ocean Model (NCOM), *Ocean Modell.*, *11*, 347–375, doi:10.1016/j.ocemod.2005.01.004.

Bingham, F. M., G. R. Foltz, and M. J. McPhaden (2010), Seasonal cycles of surface layer salinity in the Pacific Ocean, *Ocean Sci.*, *6*, 775–787, doi:10.5194/os-6-775-2010.

Boyer, T. P., et al. (2009), *World Ocean Database 2009* [DVDs], *NOAA Atlas NESDIS*, vol. 66, edited by S. Levitus, 219 pp., U.S. Gov. Print. Off., Washington, D. C.

Brainerd, K. E., and M. C. Gregg (1995), Surface mixed and mixing layer depths, *Deep Sea Res., Part I*, *42*(9), 1521–1543, doi:10.1016/0967-0637(95)00068-H.

Carnes, M., R. W. Helber, C. N. Barron, and J. M. Dastugue (2010), Validation test report for GDEM4, *Rep. NRL/MR/7330-10-9271*, Space and Nav. Warfare Syst. Command, Arlington, Va. [Available at http://www7320.nrlssc.navy.mil/pubs.php].

Carton, J. A., S. A. Grodsky, and H. Liu (2008), Variability of the oceanic mixed layer, 1960–2004, *J. Clim.*, *21*, 1029–1047, doi:10.1175/2007JCLI1798.1.

Colbo, K., and R. Weller (2007), The variability and heat budget of the upper ocean under the Chile-Peru stratus, *J. Mar. Res.*, *65*, 607–637.

Cronin, M. F., and M. J. McPhaden (2002), Barrier layer formation during westerly wind bursts, *J. Geophys. Res.*, *107*(C12), 8020, doi:10.1029/2001JC001171.

de Boyer Montégut, C., G. Madec, A. S. Fischer, A. Lazar, and D. Iudicone (2004), Mixed layer depth over the global ocean: An examination of profile data and a profile-based climatology, *J. Geophys. Res.*, *109*, C12003, doi:10.1029/2004JC002378.

de Boyer Montégut, C., J. Mignot, A. Lazar, and S. Cravatte (2007), Control of salinity on the mixed layer depth in the world ocean: 1. General description, *J. Geophys. Res.*, *112*, C06011, doi:10.1029/2006JC003953.

Feng, M., R. Lukas, P. Hacker, R. A. Weller, and S. P. Anderson (2000), Upper-ocean heat and salt balances in the western equatorial Pacific in response to the intraseasonal oscillation during TOGA COARE, *J. Clim.*, *13*, 2409–2427, doi:10.1175/1520-0442(2000)013<2409:UOHASB>2.0.CO;2.

Ferrari, R., and F. Paparella (2003), Compensation and alignment of thermohaline gradients in the ocean mixed layer, *J. Phys. Oceanogr.*, *33*, 2214–2223, doi:10.1175/1520-0485(2003)033<2214:CAAOTG>2.0.CO;2.

Flament, P. (2002), A state variable for characterizing water masses and their diffusive stability: Spiciness, *Prog. Oceanogr.*, *54*, 493–501, doi:10.1016/S0079-6611(02)00065-4.

Girishkumar, M. S., M. Ravichandran, M. J. McPhaden, and R. R. Rao (2011), Intraseasonal variability in barrier layer thickness in the south central Bay of Bengal, *J. Geophys. Res.*, *116*, C03009, doi:10.1029/2010JC006657.

Helber, R. W., C. N. Barron, M. R. Carnes, and R. A. Zingarelli (2008), Evaluating the sonic layer depth relative to the mixed layer depth, *J. Geophys. Res.*, *113*, C07033, doi:10.1029/2007JC004595.

Holte, J., and L. Talley (2009), A new algorithm for finding mixed layer depths with applications to Argo data and subantarctic mode water formation, *J. Atmos. Oceanic Technol.*, *26*, 1920–1939, doi:10.1175/2009JTECHO543.1.

Huyer, A., P. A. Wheeler, P. T. Strub, R. L. Smith, R. Letelier, and P. M. Kosro (2007), The Newport line off Oregon—Studies in the north east Pacific, *Prog. Oceanogr.*, *75*, 126–160, doi:10.1016/j.pocean.2007.08.003.

Johnston, T. M. S., and D. L. Rudnick (2009), Observations of the transition layer, *J. Phys. Oceanogr.*, *39*, 780–797, doi:10.1175/2008JPO3824.1.

Kantha, L. H., and C. A. Clayson (2000), *Small Scale Processes in Geophysical Fluid Flows*, Academic, San Diego, Calif.

Kara, A. B., P. A. Rochford, and H. E. Hurlburt (2000a), An optimal definition for ocean mixed layer depth, *J. Geophys. Res.*, *105*(C7), 16,803–16,821, doi:10.1029/2000JC900072.

Kara, A. B., P. A. Rochford, and H. E. Hurlburt (2000b), Mixed layer depth variability and barrier layer formation over the North Pacific Ocean, *J. Geophys. Res.*, *105*(C7), 16,783–16,801, doi:10.1029/2000JC900071.

Kara, A. B., R. W. Helber, and A. J. Wallcraft (2010), Evaluations of threshold and curvature mixed layer depths by various mixing schemes in the Mediterranean Sea, *Ocean Modell.*, *34*, 166–184, doi:10.1016/j.ocemod.2010.05.006.

Levitus, S., J. I. Antonov, T. P. Boyer, H. E. Garcia, and R. A. Locarnini (2005), Linear trends of zonally averaged thermosteric, halosteric, and total steric sea level for individual ocean basins and the world ocean, (1955–1959)–(1994–1998), *Geophys. Res. Lett.*, *32*, L16601, doi:10.1029/2005GL023761.

Liu, H., S. A. Grodsky, and J. A. Carton (2009), Observed subseasonal variability of oceanic barrier and compensated layers, *J. Clim.*, *22*, 6104–6119, doi:10.1175/2009JCLI2974.1.

Lorbacher, K., D. Dommenget, P. P. Niiler, and A. Köhl (2006), Ocean mixed layer depth: A subsurface proxy of ocean-atmosphere variability, *J. Geophys. Res.*, *111*, C07010, doi:10.1029/2003JC002157.

Lukas, R., and E. Lindstrom (1991), The mixed layer of the western equatorial Pacific Ocean, *J. Geophys. Res.*, *96*, suppl., 3343–3357.

Mignot, J., C. de Boyer Montégut, A. Lazar, and S. Cravatte (2007), Control of salinity on the mixed layer depth in the world ocean: 2. Tropical areas, *J. Geophys. Res.*, *112*, C10010, doi:10.1029/2006JC003954.

Mignot, J., C. de Boyer Montégut, and M. Tomczak (2009), On the porosity of barrier layers, *Ocean Sci.*, *5*, 379–387.

Ren, L., and S. C. Riser (2009), Seasonal salt budget in the northeast Pacific Ocean, *J. Geophys. Res.*, *114*, C12004, doi:10.1029/2009JC005307.

Roemmich, D., and J. Gilson (2009), The 2004–2008 mean and annual cycle of temperature, salinity, and steric height in the global ocean from the Argo Program, *Prog. Oceanogr.*, *82*, 81–100, doi:10.1016/j.pocean.2009.03.004.

Rudnick, D. L., and J. P. Martin (2002), On the horizontal density ratio in the upper ocean, *Dyn. Atmos. Oceans*, *36*, 3–21, doi:10.1016/S0377-0265(02)00022-2.

Sprintall, J., and M. Tomczak (1992), Evidence of the barrier layer in the surface layer of the tropics, *J. Geophys. Res.*, *97*, 7305–7316, doi:10.1029/92JC00407.

Toniazzo, T., C. R. Mechoso, L. C. Shaffrey, and J. M. Slingo (2010), Upper-ocean heat budget and ocean eddy transport in the south-east Pacific in a high-resolution coupled model, *Clim. Dyn.*, *35*, 1309–1329, doi:10.1007/s00382-009-0703-8.

Wijesekera, H. W., and M. C. Gregg (1996), Surface layer response to weak winds, westerly bursts, and rain squalls in the western Pacific Warm Pool, *J. Geophys. Res.*, *101*(C1), 977–997, doi:10.1029/95JC02553.

Yeager, S. G., and W. G. Large (2007), Observational evidence of winter spice injection, *J. Phys. Oceanogr.*, *37*, 2895–2919, doi:10.1175/2007JPO3629.1.

Yu, L., and R. A. Weller (2007), Objectively analyzed air-sea heat fluxes for the global ice-free oceans (1981–2005), *Bull. Am. Meteorol. Soc.*, *88*, 527–539, doi:10.1175/BAMS-88-4-527.

Zheng, Y., G. N. Kiladis, T. Shinoda, E. J. Metzger, H. E. Hurlburt, J. Lin, and B. S. Giese (2010), Upper-ocean processes under the stratus cloud

deck in the southeast Pacific Ocean, *J. Phys. Oceanogr.*, *40*, 103–120, doi:10.1175/2009JPO4213.1.

C. N. Barron, M. R. Carnes, R. W. Helber, H. E. Hurlburt, and J. G. Richman, Ocean Dynamics and Prediction, Naval Research Laboratory, 1009 Balch Blvd., Stennis Space Center, MS 39529, USA. (robert.helber@nrlssc.navy.mil)

T. Boyer, National Oceanographic Data Center, NOAA, 1315 East West Hwy., Silver Spring, MD 20910-3282, USA.